## Results

Activation of NKT cells by ES-DC pulsed with α-GalCer

Mouse splenic DC and BM-DC loaded with α-GalCer have been reported to efficiently stimulate NKT cells, resulting in the rapid induction of NK cell-like cytolytic activity and the production of cytokines such as IL-4 and IFN-γ.[2,3] We examined whether ES-DC loaded with α-GalCer had the capacity to activate NKT cells, as naturally occurring DC do.

TT2 ES cell-derived non-transfectant ES-DC (ES-DC-TT2) or BM-DC were preincubated with α-GalCer, and then cocultured with splenic T cells isolated from syngeneic CBF1 mice. After 24 h, the cultured cells were recovered and their cytolytic activity against YAC-1 target cells was analyzed by a ⁵¹Cr-release assay. The results shown in Fig. 1a indicate that a significant cytotoxity against YAC-1 cells was
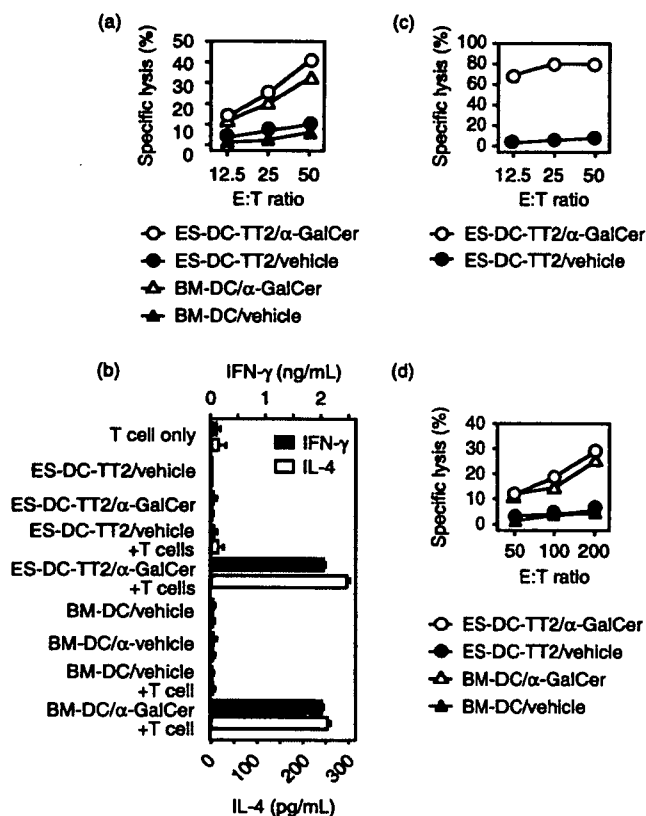
Fig. 1. Activation of NKT cells by the α-GalCer-loaded ES-DC. (a) ES-DC-TT2 or BM-DC were loaded with either α-GalCer (100 ng/mL) or vehicle (Polysorbate-20) alone for 22 h, washed extensively, and cocultured with splenic T cells of syngeneic CBF1 mice (5×10^4 DC + 2.5×10^5 T cells/well in 24-well culture plates). After 24 h of culture, the cells were recovered and the cytotoxic activity of the harvested cells against YAC-1 cells (1×10^4 cells) was analyzed using a 4-h Cr-release assay at the effector : target (E : T) ratios indicated. (b) Amounts of IL-4 and IFN-γ in the supernatant collected at the end of the 24-h coculture were quantified by ELISA. The results are expressed as the mean cytokine production of triplicate assays + SD. (c) The coculture was extended to 5 days and the killing activity of resultant cells was analyzed as in (a). (d) ES-DC or BM-DC were cultured in the presence of either α-GalCer (100 ng/mL) or vehicle alone for 18 h, washed, and injected i.p. into syngeneic CBF1 mice (1×10^6 cells/mouse). After 24 h, spleen cells were isolated from the mice and their cytotoxic activity against YAC-1 cells was analyzed as in (a). The results are expressed as the mean specific lysis of triplicate assays. The SD of triplicates were less than 2%.

induced in the splenic T cell preparations by coculture with ES-DC loaded with α-GalCer, in comparison to the coculture with ES-DC loaded with vehicle alone. The cytotoxic activity induced by α-GalCer-loaded ES-DC-TT2 was comparable to that induced by α-GalCer-loaded BM-DC (Fig. 1a). As shown in Fig. 1b, IL-4 and IFN-γ were produced by splenic T cells cocultured with α-GalCer-loaded BM-DC or ES-DC, and a similar amount of the cytokines was produced in the culture with BM-DC and ES-DC preloaded with α-GalCer. If the coculture of T cells with α-GalCer-loaded ES-DC was extended to 5 days, the induced killing activity (Fig. 1c) and the amount of IL-4 and IFN-γ produced was increased in parallel (data not shown).

We next analyzed the capacity of α-GalCer-loaded ES-DC to activate NKT cells in vivo. ES-DC-TT2 or BM-DC were preloaded with α-GalCer or vehicle alone in the same way as described above and i.p. injected into the syngeneic CBF1 mice. After 24 h, the mice were killed and the cytotoxic activity of whole spleen cells against YAC-1 cells was analyzed. As shown in Fig. 1d, a significant degree of cytotoxic activity was induced in the spleen cells by transfer of ES-DC loaded with α-GalCer, but it was not induced by the transfer of those loaded with vehicle alone. The capacity to evoke YAC-1 cell-killing activity of ES-DC and that of BM-DC was similar also in vivo. The activated NKT cells are known to activate the cytotoxic activity of NK cells.[22] It is therefore possible that the cytotoxic activity observed in these assays were mostly mediated by NK cells secondarily stimulated by NKT cells. Even so, these data collectively demonstrate that ES-DC had the capacity to present α-GalCer to activate NKT cells, and the capacity was similar to that of BM-DC both in vitro and in vivo.

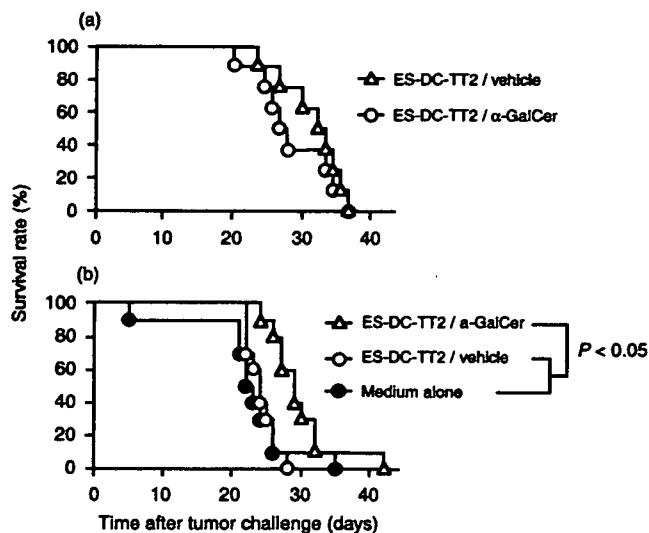### Anti-tumor effect of α-GalCer-loaded ES-DC

We assessed whether the activation of NKT cells in vivo by α-GalCer-loaded ES-DC had any therapeutic effect against the tumor cells growing in vivo. MO4, originating from NK-sensitive B16 melanoma cells, were injected s.c. into the left flank region of mice and, 3 days later, the mice were treated with an i.p. injection of ES-DC-TT2 loaded with α-GalCer or vehicle alone. As shown in Fig. 2a, ES-DC loaded with α-GalCer did not show any therapeutic effect in this s.c. tumor model.

We next investigated the effect of α-GalCer-loaded ES-DC in the peritoneally disseminated tumor model. MO4 cells were injected i.p. into mice and, 3 days later, the mice were treated with an i.p. injection of ES-DC loaded with either α-GalCer or vehicle alone. As shown in Fig. 2b, which indicated the survival rate of the treated mice, the injection of ES-DC-TT2 loaded with α-GalCer elicited a significant ($P < 0.05$) but limited protective effect against the i.p. disseminated tumor cells.

Synergic therapeutic effect of α-GalCer-activated NKT cells and antigen-specific T cells against peritoneally disseminated tumor cells
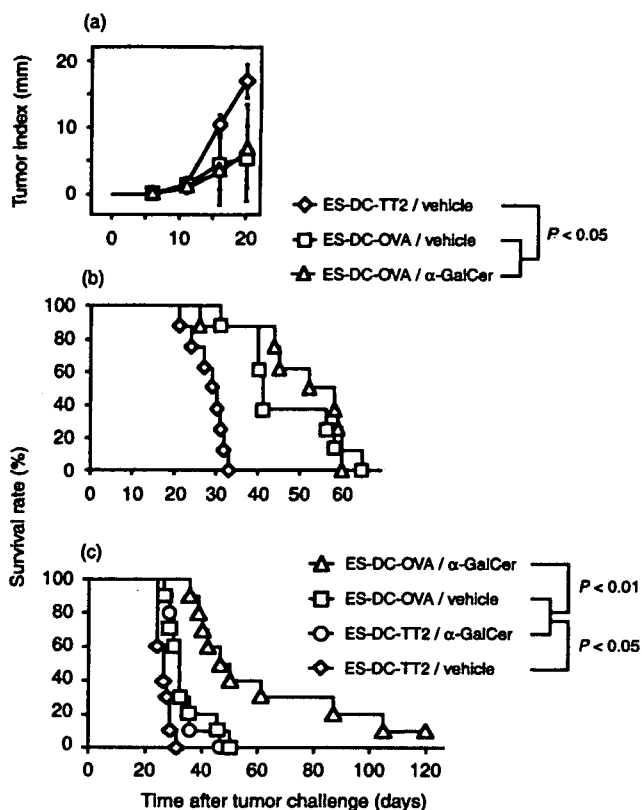
In a previous study, we demonstrated that the in vivo transfer of ES-DC-OVA effectively primed OVA-specific CTL and induced protection against a subsequent challenge with s.c. injected MO4 cells expressing OVA.[16] We investigated

Fig. 2. Anti-tumor effect of *in vivo*-transferred α-GalCer-loaded ES-DC. The mice were (a) inoculated s.c. with MO4 cells (3×10^5 cells/mouse) to the left flank region or (b) inoculated i.p. with MO4 cells (1×10^5 cells/mouse). After 3 days, the mice were treated with i.p. injection of ES-DC-TT2 (1×10^5 cells/mouse) loaded with α-GalCer, vehicle alone or medium alone, and the mouse survival rate was monitored ($n = 10$ per group). In (b), the survival rate of the α-GalCer-loaded ES-DC-TT2-treated group was higher than that of the other two groups and the difference was statistically significant. Data are representative of four independent and reproducible experiments.


Fig. 3. Synergic effect of α-GalCer loading and the expression of tumor antigen on the protection against tumors induced by ES-DC. MO4 cells (3×10^5 cells/mouse) were injected s.c. into the left flank region of the mice and, 3 days later, the mice were treated with an i.p. injection of ES-DC-TT2 (1×10^5 cells/mouse) loaded with vehicle alone, ES-DC-TT2 loaded with α-GalCer, or ES-DC-OVA loaded with α-GalCer. After that, the tumor sizes were determined (a) and survival rate was monitored (b). Both the differences in tumor index (a) and in mouse survival rate (b) between the vehicle-loaded ES-DC-TT2-treated group and other two groups were statistically significant. (c) MO4 cells (1×10^5 cells/mouse) were injected i.p. into the mice and, 3 days later, the mice were treated with an i.p. injection of ES-DC-OVA or ES-DC-TT2 (1×10^5 cells/mouse) loaded with α-GalCer or vehicle alone. Thereafter, the mouse survival rate was monitored. The survival rate of the α-GalCer-loaded ES-DC-OVA-treated group was higher than that of the other groups and the difference was statistically significant. The survival rates of the vehicle-loaded ES-DC-OVA-treated group and α-GalCer-loaded ES-DC-TT2-treated group were higher than that of vehicle-loaded ES-DC-TT2-treated group and the difference was statistically significant. Each group included 10 mice. Data are representative of three independent and reproducible experiments.

whether the loading of α-GalCer to ES-DC-OVA before *in vivo* transfer would enhance the therapeutic effect against pre-established MO4 tumor. The mice were challenged s.c. with MO4 cells, and then 3 days later they were treated by i.p. injection of ES-DC-OVA preloaded with α-GalCer or vehicle alone. As shown in Fig. 3a,b, compared to the transfer of ES-DC-TT2, the transfer of ES-DC-OVA, loaded with either α-GalCer or vehicle alone, elicited a significant antitumor effect in this therapeutic model, as observed in the previously reported prevention (prophylactic) model.[16] However, the loading of α-GalCer to ES-DC-OVA did not improve the effect, based on either the tumor growth or the mouse survival time (Fig. 3a,b). These results suggest that the activation of NKT cells by α-GalCer loaded to ES-DC does not enhance the therapeutic effect of antigen-specific T cells against s.c. growing tumor cells.

We next investigated the effect of transfer of α-GalCer-loaded ES-DC-OVA against peritoneally disseminated tumor cells. Mice were i.p. inoculated with MO4 cells and 3 days later they were treated by an i.p. injection of ES-DC-OVA loaded with α-GalCer or vehicle alone, or ES-DC-TT2 loaded with vehicle alone. As shown in Fig. 3c, the therapeutic effect of the transfer of ES-DC-OVA loaded with vehicle alone was significant ($P < 0.05$) in comparison to the treatment with ES-DC-TT2 loaded with vehicle alone, but the effect was less marked than the effect observed in the s.c. growing tumor model (Fig. 3b). In contrast, the treatment with ES-DC-OVA loaded with α-GalCer elicited a potent effect to prolong the survival time of the mice. Given that the antitumor effect elicited by α-GalCer-loaded non-transfectant ES-DC was also limited (Figs 2b,3c), these results indicate

that the NKT cells activated by α-GalCer presented by ES-DC and OVA-specific CTL primed by OVA antigen presented by the same ES-DC acted synergistically to protect the mice.

Subsets of effector cells contributing to the antitumor effect induced by α-GalCer-loaded ES-DC that expressed a model tumor antigen

To determine the effector cells exhibiting the observed antitumor effect induced by adoptive transfer of α-GalCer-loaded ES-DC expressing OVA, we carried out depletion experiments by injecting the mice with Abs specific to several subsets of effector cells during the tumor cell challenge and treatment with ES-DC. Figure 4a shows the
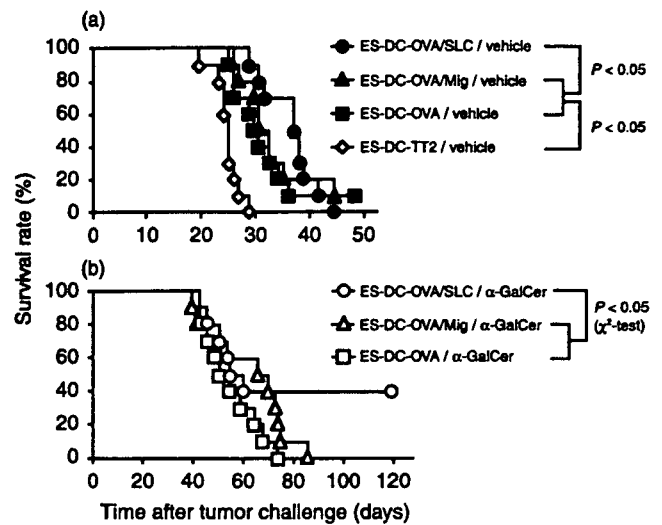
(a)

(b)

Time after tumor challenge (days)
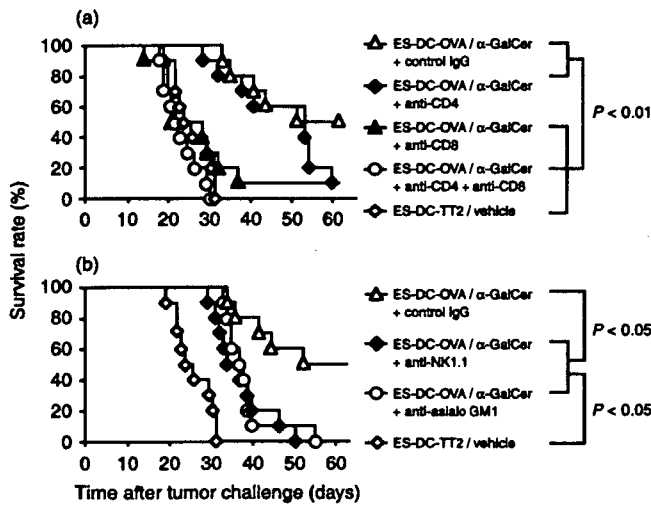
Fig. 4. Effector cells involved in the antitumor effect exerted by adoptive transfer of α-GalCer-loaded, antigen-expressing ES-DC. The mice were challenged i.p. with 1×10^5 MO4 cells on day 0 and injected i.p. with 1×10^5 ES-DC-OVA preloaded with α-GalCer on day 3. To deplete the specific types of cells, the mice were given i.p. injections of mAb or polyclonal rabbit anti-asialo GM1 Ab. The effect of the injection of anti-CD4, anti-CD8, or a combination of these two Abs is shown in (a). The effect of anti-NK1.1 or rabbit anti-asialo GM1 Ab is shown in (b). As a control, the survival of the mice treated with normal rat IgG is shown in both (a) and (b). Each group included 10 mice. In (a), the survival rates of α-GalCer-loaded ES-DC-OVA plus control IgG-treated group and α-GalCer-loaded ES-DC-OVA plus anti-CD4-treated group were higher than those of the other three groups and the difference was statistically significant. In (b), the survival rates of α-GalCer-loaded ES-DC-OVA plus anti-NK1.1 or anti-asialo GM1-treated groups and those of the other two groups were statistically different. The experiment was carried out once.

(a)

(b)

Time after tumor challenge (days)

Fig. 5. Enhanced antitumor effect elicited by α-GalCer-loaded ES-DC expressing SLC along with OVA. (a) MO4 cells (1×10^5 cells/mouse) were injected i.p. into the mice and, 3 days later, the mice were treated with i.p. injection of ES-DC-TT2, ES-DC-OVA, ES-DC-OVA/Mig, or ES-DC-OVA/SLC (1×10^5 cells/mouse), all loaded with vehicle only. Thereafter, the survival rate of the mice was monitored. The differences in the survival rate between ES-DC-OVA/Mig-treated or ES-DC-OVA-treated group and the other two groups were statistically significant. (b) The mice were challenged with MO4 cells as in (a) and treated with either ES-DC-OVA, ES-DC-OVA/SLC or ES-DC-OVA/Mig, all loaded with α-GalCer. The frequency of mice from the ES-DC-OVA/SLC-treated group surviving for more than 100 days (four out of 10 mice) was significantly higher than that of the other two groups (0 out of 10 mice in each group), according to the χ^2-test. The experiment was carried out once.

effect of the injection of anti-CD4 or anti-CD8 mAbs or a combination of these two mAbs. The injection of anti-CD8 mAb almost totally abrogated the effect of the treatment with the ES-DC, thus suggesting that CD8$^+$ OVA-specific CTL played an important role in protecting the mice from the tumor. Compared to the effect of anti-CD8 mAb, the injection of anti-CD4 mAb had far less influence on the protective effect against the tumor, thus indicating the function of CD4$^+$ helper T cells to be not essential.

Figure 4b shows the effect of the injection of rabbit anti-asialo GM1 Ab, depleting NK cells, and also that of anti-NK1.1 mAb, depleting both NK and NKT cells. Treatment with either of these two kinds of Ab decreased the effect of α-GalCer-loaded ES-DC-OVA to a level similar to that elicited by vehicle-loaded ES-DC-OVA. These results indicate that NK cells played an essential role in the enhanced antitumor effect caused by the activation of NKT cells by α-GalCer.

Enhanced antitumor effect elicited by α-GalCer-loaded ES-DC expressing SLC along with OVA

We previously found that the coexpression of SLC or Mig, T cell-attracting chemokines that natural DC do not produce, along with OVA by ES-DC significantly enhanced their capacity to prime OVA-specific CTL and also to induce a protective immunity against s.c. injected MO4 cells.[16] A recent study revealed that these two chemokines induced chemotaxis not only of conventional T cells but also of some

subpopulations of the NK cells and NKT cells.[10–12,23] We therefore examined whether the coexpression of such chemokine by ES-DC expressing OVA would also have an enhancing effect in protection against the i.p. growing MO4 cells.

We first assessed the effect of the expression of such chemokines by ES-DC without preloading with α-GalCer. We analyzed the capacity of ES-DC-OVA/SLC or ES-DC-OVA/Mig, ES-DC expressing OVA simultaneously with SLC or Mig, to induce protection against i.p. disseminated MO4 cells, comparing the capacity with that of ES-DC-OVA. The effect elicited by ES-DC-OVA/Mig was not higher than that elicited by ES-DC-OVA. Thus, the expression of Mig did not enhance the antitumor effect (Fig. 5a). However, expression of SLC by ES-DC did enhance the protective effect, although the effect of SLC in this i.p. tumor model was less evident than that observed in the s.c. tumor model reported previously.[16]

We next evaluated the effect of the expression of either SLC or Mig on the antitumor effect elicited by α-GalCer-loaded ES-DC-OVA. α-GalCer ES-DC-OVA/Mig and α-GalCer ES-DC-OVA exhibited a similar degree of protection, thus indicating that the coexpression of Mig by α-GalCer-loaded ES-DC-expressing OVA did not have any additive effect (Fig. 5b). In contrast, α-GalCer-loaded ES-DC-OVA/SLC exhibited a far more potent protective effect than α-GalCer ES-DC-OVA/Mig or α-GalCer ES-DC-OVA did. We observed that 40% of the mice treated with α-GalCer-loaded ES-DC-OVA/SLC completely rejected the tumor cells (Fig. 5b). These results suggest that the SLC produced by

ES-DC augmented the synergic effect of antigen-reactive CTL, α-GalCer-activated NKT cells, and probably NK cells.

As we reported previously,[16] coexpression of SLC along with OVA in ES-DC enhanced the capacity of ES-DC to prime OVA-specific CTL upon *in vivo* transfer. The data shown in the Fig. 5a also indicate that coexpression of SLC enhanced the capacity of ES-DC to induce antitumor immunity mediated by OVA-specific CTL in the absence of α-GalCer. To assess the effect of SLC produced by ES-DC on the activation of NKT or NK cells, we compared the capacity of α-GalCer-loaded ES-DC-OVA and α-GalCer-loaded ES-DC-OVA/SLC to stimulate NKT cells by an experiment similar to that shown in Fig. 1d. As a result, we observed that the capacity of α-GalCer-loaded ES-DC to induce YAC-1 cell-killing activity was not enhanced by expression of SLC (data not shown). Thus, effect of SLC produced by ES-DC to enhance the activation of NKT and NK cells was not detected at least by this short-term (24 h) assay. Based on these observations, it may be considered that the expression of SLC by ES-DC dominantly enhanced the activation of antigen-specific CTL rather than NKT or NK cells.

Discussion

In the present study, we evaluated the effect of loading α-GalCer to ES-DC expressing a model tumor antigen on their capacity to induce antitumor immunity. Upon loading with α-GalCer, ES-DC had a capacity comparable to that of BM-DC to stimulate NKT cells (Fig. 1). The *in vivo* administration α-GalCer-loaded non-transfectant ES-DC had some antitumor effect in an i.p. disseminated tumor model but not in an s.c. growing tumor model (Fig. 2). The difference in the effect of loading of α-GalCer to ES-DC in between the two models may be accounted for by the tissue distribution of NKT cells. NKT cells localize mainly in the liver, lung, spleen, bone marrow and peritoneal cavity.[6,11,24,25] In parallel with these observations, the loading of α-GalCer to ES-DC-OVA enhanced their antitumor effect against i.p. disseminated but not s.c. growing MO4 tumor cells (Fig. 3).

In a previous study, we observed that the protective effect against s.c. growing MO4 cells by transfer of ES-DC-OVA was almost totally abrogated by the depletion of either of CD4 or CD8 T cells.[16] In contrast, in the present study, the depletion of CD8+ T cells but not CD4+ T cells diminished the antitumor effect against i.p. MO4 cells elicited by α-GalCer-loaded ES-DC-OVA (Fig. 4a). These results indicate that CTL play a pivotal role in both conditions, and that CD4+ T helper cells were not essential in the protective immunity against i.p. tumor cells on the occasion of simultaneous activation of NKT cells. The reason for the dispensability of CD4+ T helper cells may be that NKT cells and NK cells, secondarily activated by NKT cells, provide help to OVA-specific CTL.[26] The data shown in Fig. 4b revealed that the depletion of NK cells decreased the effect of α-GalCer-loaded ES-DC-OVA to a degree similar to that elicited by vehicle-loaded ES-DC-OVA, indicating that NK cells played an essential role in the enhancement of the antitumor effect obtained by loading α-GalCer to ES-DC-OVA. Collectively, CD8+ CTL, NKT cells and NK cells played essential roles in the antitumor effect obtained by α-GalCer to ES-DC expressing
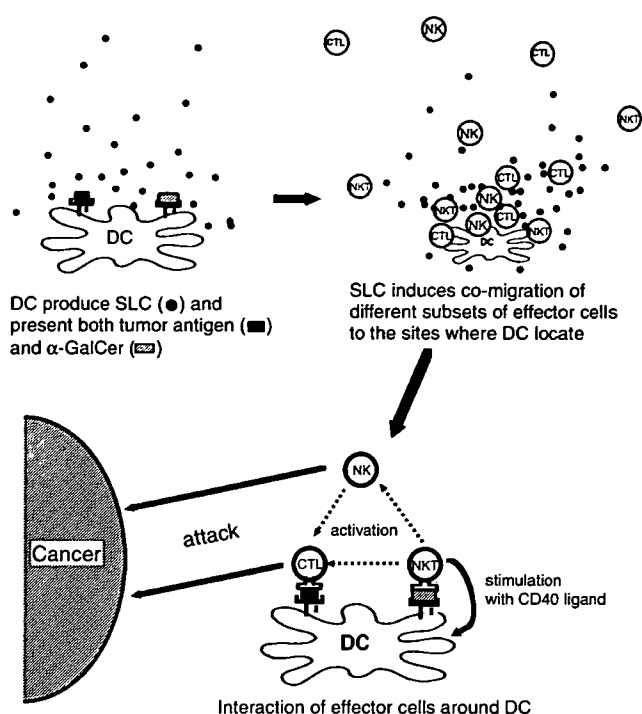
Fig. 6. A schematic depiction of the enhanced cross-talk of different subsets of effector cells induced by α-GalCer-loaded ES-DC expressing OVA plus SLC. SLC secreted by ES-DC induces the comigration of different subsets of effector cells, including NKT cells, NK cells and antigen-specific T cells, to the sites where the injected ES-DC are located. The effector cells of both innate and acquired immunity gathered around ES-DC, which present both α-GalCer and tumor antigen, thus closely interacting to develop a potent antitumor immunity.

the antigen (Fig. 6). Presumably, the sequential stimulation of NKT cells and NK cells augmented the antitumor effect of OVA-specific CTL[9] and probably the interactions of effector cells were mediated by IFN-γ and IL-2.[22,27-31]

The data shown in Fig. 5b indicate that the expression of SLC by ES-DC enhanced the antitumor effect induced by the transfer of α-GalCer-loaded ES-DC expressing OVA. SLC has been reported to attract not only conventional T cells and DC but also NKT cells.[10,23] SLC also induces chemotaxis of CD56bright CD16− NK cells and has a costimulatory effect on the proliferation of NK cells.[32] Thus, SLC probably induced the comigration of conventional T cells, NKT cells and NK cells to the sites where ES-DC were located, and, as a result, the close interaction of such multiple subsets of effector cells may have occurred (Fig. 6).

In the past decade, α-GalCer has been attracting attention as a novel immunostimulatory reagent for antitumor therapy. Based on the promising results of preclinical studies demonstrating antitumor effects of α-GalCer,[2,25,33] several phase I clinical studies on anticancer immunotherapy by the direct intravenous administration of α-GalCer or the administration of α-GalCer-loaded DC have been carried out.[34-37] Although the activation and expansion of NKT cells by the administration of α-GalCer has been observed, the results seemed to be unsatisfactory from the viewpoint of the clinical effect. The present study demonstrated that α-GalCer is useful for induction

of immunity against peritoneally disseminated tumor cells, especially when it is loaded to DC genetically engineered to express tumor antigen. Although metastasis of melanoma to visceral organ sites is observed frequently in patients with advanced (stage IV) malignant melanoma, peritoneal dissemination of melanoma is very rare. Thus, we are planning another study with more clinical relevance, using models of cancer with a high tendency to peritoneal dissemination.

In recent years, a number of tumor-associated antigens have been identified. These antigens are potentially good targets for immunotherapy. To establish truly effective anticancer immunotherapy, a method for potently polarizing the immune system toward these antigens is essential. Antitumor immunotherapy with DC loaded with HLA-binding peptides derived from tumor antigens has been tested clinically in many institutions. In most cases, the DC are generated by culture of monocytes obtained from peripheral blood of the patients. To generate a sufficient number of DC for treatment, apheresis, a procedure that is sometimes invasive for patients with advanced stages of cancer, is necessary to obtain a sufficient number of monocytes as a source for DC. In addition, the culture to generate DC should be done separately for each patient and for each treatment, and thus the procedure used at present may be too labor-intensive and expensive to be applied broadly in a practical setting. Alternately, the source of ES-DC, ES cells, have the capacity to propagate infinitely. We would thus be able to use human ES cells as an infinite source of DC. In addition, we will be able to generate genetically engineered DC without the need to use virus vectors, as mentioned above. We may thus be able to generate multiple gene-transfectant ES-DC expressing tumor antigen plus immunostimulating molecules, which could be more potent in stimulating antitumor immunity than monocyte-derived DC are.

Regarding the future clinical application of ES-DC, we recently established a method for generating ES-DC from ES cells of a non-human primate, namely the cynomolgus monkey, and also for their genetic modification (unpublished data). We believe that this method would be applicable to human ES cells, although some modifications may be necessary. Considering the future clinical application of ES-DC technology, allogenicity (i.e. differences in the genetic background) between patients to be treated and ES cells as a source for DC may cause problems. However, it is expected that human ES cells sharing some HLA alleles with patients will be available for most cases. We recently found that antigen-expressing ES-DC potently primed antigen-specific CTL after the transfer to semiallogeneic mice sharing some MHC alleles with the ES-DC, and protected the recipient mice from subsequent challenge with tumor cells bearing the antigen.[38] CD1d is monomorphic and thus a CD1d-α-GalCer-complex on ES-DC can stimulate the NKT cells of any recipients. α-GalCer would thus be an ideal adjuvant to enhance the immune response toward the tumor antigens presented by ES-DC.

Acknowledgments

References

1 Kitamura H, Iwakabe K, Yahata T et al. The natural killer T (NKT) cell ligand alpha-galactosylceramide demonstrates its immunopotentiating effect by inducing interleukin (IL)-12 production by dendritic cells and IL-12 receptor expression on NKT cells. J Exp Med 1999; 189: 1121–8.

2 Toura I, Kawano T, Akutsu Y, Nakayama T, Ochiai T, Taniguchi M. Cutting edge: inhibition of experimental tumor metastasis by dendritic cells pulsed with α-galactosylceramide. J Immunol 1999; 163: 2387–91.

3 Fujii S, Shimizu K, Kronenberg M, Steinman RM. Prolonged IFN-γ-producing NKT response induced with alpha-galactosylceramide-loaded DCs. Nat Immunol 2002; 3: 867–74.

4 Bezbradica JS, Stanic AK, Matsuki N et al. Distinct roles of dendritic cells and B cells in Val14Ja18 natural T cell activation in vivo. J Immunol 2005; 174: 4696–705.

5 Gonzalez-Aseguinolaza G, de Oliveira C, Tomaska M et al. α-Galactosylceramide-activated Vα 14 natural killer T cells mediate protection against murine malaria. Proc Natl Acad Sci USA 2000; 97: 8461–6.

6 Kawamura T, Seki S, Takeda K et al. Protective effect of NK1.1+ T cells as well as NK cells against intraperitoneal tumors in mice. Cell Immunol 1999; 193: 219–25.

7 Johnson TR, Hong S, Van Kaer L, Koezuka Y, Graham BS. NK T cells contribute to expansion of CD8+ T cells and amplification of antiviral immune responses to respiratory syncytial virus. J Virol 2002; 76: 4294–303.

8 Nishimura T, Kitamura H, Iwakabe K et al. The interface between innate and acquired immunity: glycolipid antigen presentation by CD1d-expressing dendritic cells to NKT cells induces the differentiation of

antigen-specific cytotoxic T lymphocytes. Int Immunol 2000; 12: 987–94.

9 Silk JD, Hermans IF, Gileadi U et al. Utilizing the adjuvant properties of CD1d-dependent NK T cells in T cell-mediated immunotherapy. J Clin Invest 2004; 114: 1800–11.

10 Kim CH, Johnston B, Butcher EC. Trafficking machinery of NKT cells: shared and differential chemokine receptor expression among V alpha 24+V beta 11+ NKT cell subsets with distinct cytokine-producing capacity. Blood 2002; 100: 11–16.

11 Liu Y, Poon RT, Hughes J, Feng X, Yu WC, Fan ST. Chemokine receptors support infiltration of lymphocyte subpopulations in human hepatocellular carcinoma. Clin Immunol 2005; 114: 174–82.

12 Thomas SY, Hou R, Boyson JE et al. CD1d-restricted NKT cells express a chemokine receptor profile indicative of Th1-type inflammatory homing cells. J Immunol 2003; 171: 2571–80.

13 Kaplan JM, Yu Q, Piraino ST et al. Induction of antitumor immunity with dendritic cells transduced with adenovirus vector-encoding endogenous tumor-associated antigens. J Immunol 1999; 163: 699–707.

14 Fairchild PJ, Brook FA, Gardner RL et al. Directed differentiation of dendritic cells from mouse embryonic stem cells. Curr Biol 2000; 10: 1515–18.

15 Senju S, Hirata S, Matsuyoshi H et al. Generation and genetic modification of dendritic cells derived from mouse embryonic stem cells. Blood 2003; 101: 3501–8.

16 Matsuyoshi H, Senju S, Hirata S, Yoshitake Y, Uemura Y, Nishimura Y. Enhanced priming of antigen-specific CTLs in vivo by embryonic stem cell-derived dendritic cells expressing chemokine along with antigenic protein: application to antitumor vaccination. J Immunol 2004; 172: 776–86.

17 Hirata S, Senju S, Matsuyoshi H, Fukuma D, Uemura Y, Nishimura Y. Prevention of experimental autoimmune encephalomyelitis by transfer of

embryonic stem cell-derived dendritic cells expressing myelin oligodendrocyte glycoprotein peptide along with TRAIL or programmed death-1 ligand. *J Immunol* 2005; **174**: 1888–97.

18 Yagi T, Tokunaga T, Furuta Y *et al*. A novel ES cell line, TT2, with high germline-differentiating potency. *Anal Biochem* 1993; **214**: 70–6.

19 Senju S, Iyama K, Kudo H, Aizawa S, Nishimura Y. Immunocytochemical analyses and targeted gene disruption of GTPBP1. *Mol Cell Biol* 2000; **20**: 6195–200.

20 Falo LD Jr, Kovacsovics-Bankowski M, Thompson K, Rock KL. Targeting antigen into the phagocytic pathway *in vivo* induces protective tumour immunity. *Nat Med* 1995; **1**: 649–53.

21 Lutz MB, Kukutsch N, Ogilvie AL *et al*. An advanced culture method for generating large quantities of highly pure dendritic cells from mouse bone marrow. *J Immunol Meth* 1999; **223**: 77–92.

22 Eberl G, MacDonald HR. Selective induction of NK cell proliferation and cytotoxicity by activated NKT cells. *Eur J Immunol* 2000; **30**: 985–92.

23 Johnston B, Kim CH, Soler D, Emoto M, Butcher EC. Differential chemokine responses and homing patterns of murine TCR alpha beta NKT cell subsets. *J Immunol* 2003; **171**: 2960–9.

24 Takeda K, Seki S, Ogasawara K *et al*. Liver NK1.1⁺ CD4⁺ alpha beta T cells activated by IL-12 as a major effector in inhibition of experimental tumor metastasis. *J Immunol* 1996; **156**: 3366–73.

25 Nakagawa R, Motoki K, Ueno H *et al*. Treatment of hepatic metastasis of the colon26 adenocarcinoma with an α-galactosylceramide, KRN7000. *Cancer Res* 1998; **58**: 1202–7.

26 Stober D, Jomantaite I, Schirmbeck R, Reimann J. NKT cells provide help for dendritic cell-dependent priming of MHC class I-restricted CD8⁺ T cells *in vivo*. *J Immunol* 2003; **170**: 2540–8.

27 Hayakawa Y, Takeda K, Yagita H *et al*. Critical contribution of IFN-γ and NK cells, but not perforin-mediated cytotoxicity, to anti-metastatic effect of α-galactosylceramide. *Eur J Immunol* 2001; **31**: 1720–7.

28 Carnaud C, Lee D, Donnars O *et al*. Cutting edge: Cross-talk between cells of the innate immune system: NKT cells rapidly activate NK cells. *J Immunol* 1999; **163**: 4647–50.

29 Smyth MJ, Crowe NY, Pellicci DG *et al*. Sequential production of interferon-γ by NK1.1⁺ T cells and natural killer cells is essential for the antimetastatic effect of α-galactosylceramide. *Blood* 2002; **99**: 1259–66.

30 Chamoto K, Takeshima T, Kosaka A *et al*. NKT cells act as regulatory cells rather than killer cells during activation of NK cell-mediated cytotoxicity by α-galactosylceramide *in vivo*. *Immunol Lett* 2004; **95**: 5–11.

31 Wesley JD, Robbins SH, Sidobre S, Kronenberg M, Terrizzi S, Brossay L. Cutting edge: IFN-γ signaling to macrophages is required for optimal Vα14i NK T/NK cell cross-talk. *J Immunol* 2005; **174**: 3864–8.

32 Robertson MJ. Role of chemokines in the biology of natural killer cells. *J Leukoc Biol* 2002; **71**: 173–83.

33 Hayakawa Y, Rovero S, Forni G, Smyth MJ. Alpha-galactosylceramide (KRN7000) suppression of chemical- and oncogene-dependent carcinogenesis. *Proc Natl Acad Sci USA* 2003; **100**: 9464–9.

34 Nieda M, Okai M, Tazbirkova A *et al*. Therapeutic activation of Vα24⁺Vβ11⁺ NKT cells in human subjects results in highly coordinated secondary activation of acquired and innate immunity. *Blood* 2004; **103**: 383–9.

35 Giaccone G, Punt CJ, Ando Y *et al*. A phase I study of the natural killer T-cell ligand α-galactosylceramide (KRN7000) in patients with solid tumors. *Clin Cancer Res* 2002; **8**: 3702–9.

36 Ishikawa A, Motohashi S, Ishikawa E *et al*. A phase I study of α-galactosylceramide (KRN7000)-pulsed dendritic cells in patients with advanced and recurrent non-small cell lung cancer. *Clin Cancer Res* 2005; **11**: 1910–17.

37 Chang DH, Osman K, Connolly J *et al*. Sustained expansion of NKT cells and antigen-specific T cells after injection of α-galactosyl-ceramide loaded mature dendritic cells in cancer patients. *J Exp Med* 2005; **201**: 1503–17.

38 Fukuma D, Matsuyoshi H, Hirata S *et al*. Cancer prevention with semi-allogeneic ES cell-derived dendritic cells. *Biochem Biophys Res Commun* 2005; **335**: 5–13.

— 303 —

Activation of Invariant Natural Killer T Cells by Synthetic Glycolipid Ligands Suppresses Autoantibody-Induced Arthritis

Shinjiro Kaieda,[1] Chiharu Tomi,[2] Shinji Oki,[2] Takashi Yamamura,[2] and Sachiko Miyake[2]

Objective. Stimulation of invariant natural killer T (iNKT) cells with SGL-S23, a novel synthetic glycolipid analog of α-galactosylceramide with an elongated sphingosine chain, has been shown to strongly suppress K/BxN serum transfer arthritis. This study was designed to evaluate the protective effects of SGL-S23 in an effector phase of arthritis.

Methods. To induce arthritis, C57BL/6 mice were injected with 150 μl of serum from K/BxN mice (KRN TCR–transgenic mice crossed with nonobese diabetic mice). Subsequently, synthetic glycolipid ligands were administered intraperitoneally twice, either 3 times starting on day 0 (the day of K/BxN serum injection) or twice starting on day 3. Neutralizing antibody against interferon-γ (IFNγ) interleukin-4 (IL-4), IL-10, or transforming growth factor β was administered 4 hours before injection of SGL-S23. Recombinant IFNγ was administered subcutaneously every day. The severity of arthritis was monitored using a macroscopic scoring system. Cytokine production and plasma histamine levels were measured by enzyme-linked immunosorbent assay.

Results. SGL-S23 strongly suppressed K/BxN serum transfer arthritis by inhibiting inflammatory cell infiltration and subsequent destruction of cartilage and bone. The inhibitory effect mediated by SGL-S23 was abolished by neutralization of IFNγ. Systemic administration of IFNγ prevented the development of inflammatory arthritis. Histamine release was suppressed by administration of SGL-S23 or IFNγ. Degranulated mast cells in the synovium were significantly reduced in SGL-S23–treated mice, suggesting that suppression of mast cell activation contributed to the inhibition of arthritis.

Conclusion. These findings suggest that activation of iNKT cells with glycolipid ligands holds promise with regard to the treatment of autoimmune diseases such as rheumatoid arthritis. SGL-S23 has clinical benefit over α-galactosylceramide since it induces a weaker cytokine production response in iNKT cells, therefore reducing potential side effects caused by excessive cytokine release.

Rheumatoid arthritis is a common autoimmune disease characterized by chronic inflammation and progressive destruction of joints. Although antigen-specific T cells in the joints have been thought to be important in inciting an inflammatory cascade, triggering activation of macrophages and synoviocytes, recent advances in antiinflammatory drugs such as anti–tumor necrosis factor (anti-TNF) agents serve as a reminder of the importance of the later inflammatory phase in the pathogenesis and control of arthritis (1,2).

K/BxN mice (KRN TCR–transgenic mice crossed with nonobese diabetic [NOD] mice) spontaneously develop a polyarthritis with many of the hallmarks of human rheumatoid arthritis, including cellular infiltration, synovial hyperplasia, and bone and cartilage destruction (3). The disease depends on recognition of glucose-6-phosphate isomerase (GPI) presented by I-A^{g7} in the periphery (4). Furthermore, arthritis can be induced in most strains of mice by transfer of K/BxN

[1]Shinjiro Kaieda, MD: National Institute of Neuroscience, National Center of Neurology and Psychiatry, Tokyo, Japan, and Kurume University School of Medicine, Kurume, Japan; [2]Chiharu Tomi, Shinji Oki, PhD, Takashi Yamamura, MD, PhD, Sachiko Miyake, MD, PhD: National Institute of Neuroscience, National Center of Neurology and Psychiatry, Tokyo, Japan.

Address correspondence and reprint requests to Sachiko Miyake, MD, PhD, Department of Immunology, National Institute of Neuroscience, National Center of Neurology and Psychiatry, 4-1-1 Ogawahigashi, Kodaira, Tokyo 187-8502, Japan. E-mail: miyake@ncnp.go.jp.

Submitted for publication August 18, 2006; accepted in revised form March 7, 2007.

mouse serum or affinity-purified anti-GPI antibodies (4,5). Recent studies with the K/BxN serum transfer model have led to new understanding of the importance of autoantibodies and mediators of innate immunity in the pathogenesis of arthritis. This adoptive transfer process requires the presence of proinflammatory cytokines such as interleukin-1 (IL-1) and TNFα and activation of alternative-pathway complement including C5a (6,7). It has also been shown that mast cells, neutrophils, macrophages, and Fcγ receptor III (FcγRIII) are critical for disease development (7–10).

CD1d-restricted invariant natural killer T (iNKT) cells are a unique subset of T cells that express an invariant T cell receptor (TCR) α-chain and recognize glycolipid antigens presented by CD1d (11,12). Invariant NKT cells are an attractive target for the development of immunotherapies, not only because they contribute to various types of immunoregulation, but also because several synthetic glycolipid ligands specifically activate these cells (13–17). The lack of polymorphism in the antigen-presenting molecule indicates that the ligand has potential for widespread use among individuals, unlike major histocompatibility complex–restricted antigens.

The glycolipid α-galactosylceramide (α-GalCer) is a synthetic glycolipid originally isolated from marine sponge *Agelas mauritianius* and used as a component of anticancer agents, and subsequently a synthetic analog of this compound, KRN7000 (referred to herein as α-GalCer), has been used in experimental studies and in several cancer clinical trials (15–20). Glycolipid α-GalCer and its analogs such as OCH, a sphingosine truncated form, have been shown to suppress autoimmune disease in animal models by inducing a Th2 response to autoantigen (13–17,21–25). In autoantibody-mediated arthritis such as the K/BxN serum transfer model, in which innate immune cells rather than lymphocytes are critical in the pathogenesis (6), iNKT cells have been shown to exaggerate the disease, probably by a mechanism other than modulation of the Th1/Th2 balance (26,27). These findings led us to test a panel of analogs of α-GalCer for their ability to suppress antibody-mediated arthritis.

In the present study, we found that activation of iNKT cells with a novel synthetic glycolipid ligand strongly suppressed K/BxN serum transfer arthritis. Furthermore, we demonstrated the critical role of interferon-γ (IFNγ) in iNKT cell–mediated inhibition of antibody-mediated inflammation.

MATERIALS AND METHODS

Mice. C57BL/6 (B6) mice were purchased from Clea (Tokyo, Japan). Jα18-knockout mice (28) were kindly provided by Dr. Masaru Taniguchi (Riken Research Center for Allergy and Immunology, Yokohama, Japan). These mice were generated on the 129 strain and backcrossed 10 times to the B6 background. KRN TCR-transgenic mice (3) were kindly provided by Drs. Christophe Benoist and Diane Mathis (Joslin Diabetes Center, Boston, MA). Animals were kept under specific pathogen–free conditions. Animal care and use were in accordance with institutional guidelines.

Glycolipids. Glycolipids SGL-S23, S25, S27, and α-GalCer (KRN7000) were synthesized by reacting 4,5-anhydro-1,3-O-benzylidene-D-arabitol with alkyl metal reagents that correspond to the length of sphingosine side chain, and performing subsequent transformations as previously described (29).

Induction of arthritis by K/BxN serum transfer. As previously described, KRN TCR-transgenic mice maintained on the B6 background were crossed with NOD mice to generate K/BxN mice, which spontaneously develop arthritis (3). K/BxN serum pools were prepared from 8-week-old arthritic mice, and arthritis was induced in B6 mice by intraperitoneal injection of 150 μl serum. Serum from nontransgenic littermate mice crossed with NOD mice (BxN mice) was used as control serum.

Clinical assessment of arthritis. Mice were examined for signs of joint inflammation, scored as follows: 0 = no change, 1 = significant swelling and redness of 1 digit, 2 = mild swelling and erythema of the limb or swelling of >2 digits, 3 = marked swelling and erythema of the limb, 4 = maximal swelling and redness of the limb and subsequent ankylosis. The macroscopic score was expressed as the sum of the scores in all paws, with a maximum possible score of 16.

Histopathologic analysis. B6 mice were killed 10 days after K/BxN serum transfer. All 4 paws were removed and then fixed in buffered formalin, decalcified, embedded in paraffin, sectioned, and stained with hematoxylin and eosin or toluidine blue. Histologic features of joint inflammation were scored as follows: 0 = normal joint, 1 = mild arthritis (minimal synovitis without cartilage/bone erosions), 2 = moderate arthritis (synovitis and erosions but joint architecture maintained), 3 = severe arthritis (synovitis, erosions, and loss of joint integrity) (30). The histologic score was expressed as the sum of the scores in all paws, with a maximum possible score of 12. Mast cells in synovium were visually assessed for intact versus degranulating phenotype, using morphologic criteria. Mast cells were identified as cells that contained toluidine blue–positive granules. Only cells in which a nucleus was present were counted. Degranulating cells were defined by the presence of granules outside the cell border with coincident vacant granule space within the cell border, as described previously (8).

In vivo antibody treatment. Mice were administered SGL-S23 at a dose of 100 μg/kg, in 3 intraperitoneal injections on day 0 (the day of immunization), day 3, and day 7 or in 2 intraperitoneal injections on day 3 and day 7. Control mice were injected with vehicle alone (10% DMSO in phosphate buffered saline [PBS]). To neutralize IFNγ, IL-4, IL-10, or transforming growth factor β (TGFβ), 500 μg of anti-IFNγ
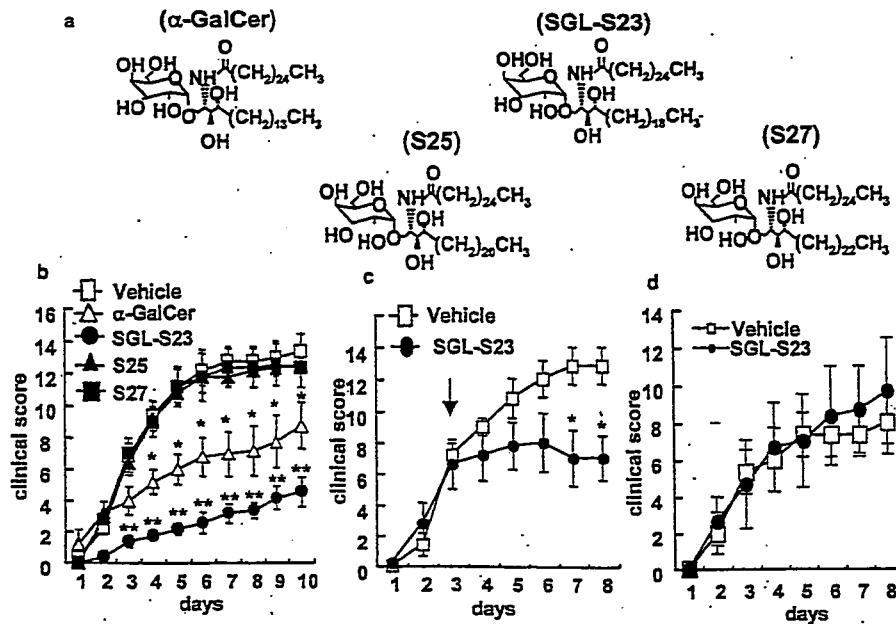
Figure 1. Effect of glycolipid antigens on K/BxN serum transfer arthritis in C57BL/6 (B6) and Jα18-knockout mice. a, Structure of the synthetic glycolipids used in this study. KRN7000 (α-GalCer) is the prototypical α-galactosylceramide and contains a C18 sphingosine base and a C26 acyl chain. SGL-S23, S25, and S27 differ from α-GalCer in the length of the sphingosine base. b, Clinical score of K/BxN serum transfer arthritis in B6 mice treated with 100 μg/kg of α-GalCer, SGL-S23, S25, S27, or vehicle 3 times, starting on the day of K/BxN serum transfer (day 0). ∗ = P < 0.05; ∗∗ = P < 0.01, versus vehicle-treated mice. c, Clinical score of K/BxN serum transfer arthritis in B6 mice treated with 100 μg/kg of SGL-S23 or vehicle twice, starting on day 3 (arrow). ∗ = P < 0.05 versus vehicle-treated mice. d, Clinical score of K/BxN serum transfer arthritis in Jα18-knockout mice treated with 100 μg/kg of SGL-S23 or vehicle 3 times, starting on day 0. Values in b–d are the mean ± SEM of 5 mice per group, from a single experiment representative of 2 similar experiments.

monoclonal antibody (mAb) (R4-6A2), anti–IL-4 mAb (11B11), anti–IL-10 mAb (JES052A5), or anti-TGFβ mAb (1D11.16.8) was injected intraperitoneally 4 hours before administration of glycolipid. Non–isotype-matched whole rat IgG or mouse IgG (Sigma, St. Louis, MO) was used as control antibody.

In vitro stimulation. Liver mononuclear cells from B6 mice were isolated by Percoll density-gradient centrifugation and stained with phycoerythrin (PE)–conjugated NK1.1 and fluorescein isothiocyanate (FITC)—conjugated CD3 mAb. Dendritic cells from spleen cells were purified using anti-CD11c microbeads (Miltenyi Biotec, Bergisch Gladbach, Germany). The purity of sorted NKT cells and dendritic cells was >95%. NKT cells were cultured for 48 hours with irradiated dendritic cells and glycolipid ligands in RPMI 1640 medium supplemented with 50 μM 2-mercaptoethanol, 2 mM L-glutamine, 100 units/ml penicillin/streptomycin, and 10% fetal calf serum. The content of cytokines in the culture supernatants was measured by cytometric bead array (BD PharMingen, San Jose, CA), and proliferative responses were assessed based on incorporation of ³H-thymidine (1 μCi/well) in the final 16 hours (analyzed with an αβ-1205 counter [Pharmacia, Uppsala, Sweden]).

Assessment of in vivo responses of iNKT cells to glycolipid antigen. B6 mice were injected intraperitoneally with 100 μg/kg of glycolipid ligands and serum was collected 6 hours and 24 hours after injection. Serum levels of IFNγ were measured by enzyme-linked immunosorbent assay (ELISA).

Flow cytometry and intracellular cytokine staining. Liver mononuclear cells harvested after stimulation with glycolipids in vivo were cultured in complete media containing GolgiStop (BD PharMingen). Cells were then incubated with Fc blocker (anti-mouse FcγIII/IIR mAb clone 2.4G2) and stained with α-GalCer–loaded Dimer X recombinant soluble dimeric mouse CD1d (BD PharMingen), washed with PBS, and then stained with FITC-conjugated mAb A85-1 (anti–mouse IgG1) and allophycocyanin (APC)–conjugated anti–TCR β-chain (BD PharMingen). Subsequently, cells were washed twice with PBS and fixed in Cytofix/Cytoperm (BD PharMingen) solution for 20 minutes at 4°C. After fixation, cells were washed with Perm/Wash (BD PharMingen) solution and resuspended in the same solution containing either PE-conjugated anti-IFNγ mAb XMG1.2 or PE-conjugated isotype control Ig, for 30 minutes at 4°C. Then samples were washed and stained cells analyzed using a FACSCalibur (Becton Dickinson, Mountain View, CA) with CellQuest software

(Becton Dickinson). Liver mononuclear cells stained with α-GalCer–loaded dimeric mouse CD1d followed by FITC-conjugated mAb A85-1 were then stained with SGL-S23–loaded dimeric mouse CD1d followed by PE-conjugated mAb A85-1 and APC-conjugated anti–TCR β-chain. PE-conjugated mAb A85-1 was confirmed not to react with the previously used α-GalCer–loaded dimeric mouse CD1d/FITC-conjugated A85-1 mAb (results not shown).

Measurement of plasma histamine concentrations. Five minutes after intravenous administration of 200 μl K/BxN serum, BxN serum, or PBS, blood from the mice was collected into heparin-containing microtubes. Samples with obvious hemolysis during blood collection were excluded in order to avoid an artificial increase in the histamine concentration due to platelet lysis. The plasma level of histamine was examined by ELISA (Research Diagnostics, Flanders, NJ).

Statistical analysis. The nonparametric Mann-Whitney U test was used to calculate significance levels for all measurements. P values less than 0.05 were considered significant.

RESULTS

Activation of iNKT cells by synthetic glycolipid ligands suppresses K/BxN serum transfer arthritis. Through screening of a panel of analogs of α-GalCer for the ability to suppress K/BxN serum transfer arthritis, we found that (2S,3S,4R)-1-O-(α-D-galactopyranosyl)-N-hexacosanoyl-2-amino-1,3,4-tricosanetriol, an α-GalCer analog with a 5-carbon longer sphingosine base compared with α-GalCer (referred to as SGL-S23 [suppressor glycolipid S23]) (Figure 1a) had a strong ability to suppress arthritis. Administration of SGL-S23 almost completely inhibited the development of arthritis (Figure 1b); α-GalCer also inhibited arthritis, but to a lesser extent. Arthritis was not suppressed by (2S,3S,4R)-1-O-(α-D-galactopyranosyl)-N-hexacosanoyl-2-amino-1,3,4-pentacosanetriol or (2S,3S,4R)-1-O-(α-D-galactopyranosyl)-N-hexacosanoyl-2-amino-1,3,4-heptacosanetriol, α-GalCer analogs with a 7- or 9-carbon longer sphingosine base (referred to as S25 and S27, respectively) (Figures 1a and b).

To examine the potential therapeutic effect of SGL-S23 on established arthritis, we injected SGL-S23 on day 3 after serum injection, when arthritis had already developed (Figure 1c). In contrast to findings in vehicle-treated mice, in which the severity of arthritis gradually increased, disease severity did not increase, and even decreased, in SGL-S23–treated mice. These results suggest that SGL-S23 has a therapeutic effect in established arthritis.

To confirm that SGL-S23–mediated suppression of K/BxN serum transfer arthritis depends on iNKT cells, we examined the ability of SGL-S23 to modulate
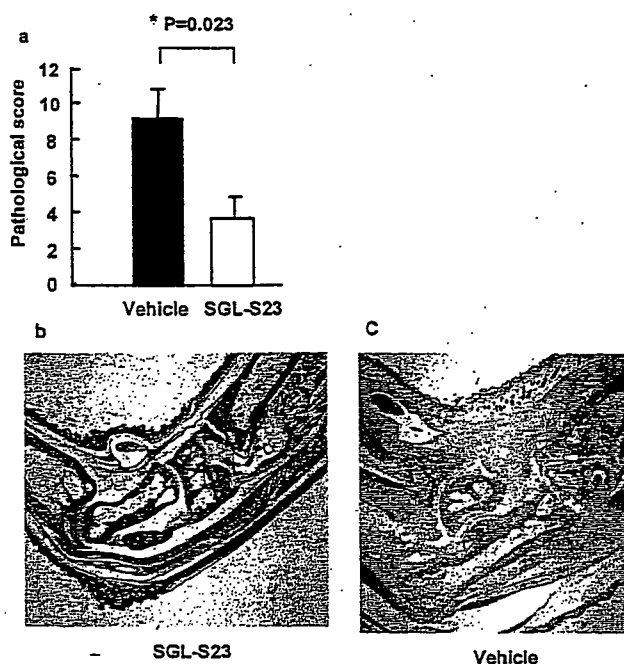
Figure 2. Histopathologic assessment of arthritic joints. **a,** Quantification of histopathologic findings in the joints of C57BL/6 mice, 10 days after K/BxN serum transfer. Mice were treated with 100 μg/kg of SGL-S23 or vehicle 3 times, starting on the day of serum transfer. Values are the mean and SEM of 3 mice per group, from a single experiment representative of 2 similar experiments. **b** and **c,** Histopathologic findings in the joints of representative SGL-S23–treated (b) and vehicle-treated (c) mice (hematoxylin and eosin stained; original magnification × 40).

disease in J$_α$18-knockout mice, in which iNKT cells are absent (28). Administration of SGL-S23 did not modulate the clinical course of arthritis induced in these mice by injection of K/BxN serum, compared with that in mice treated with vehicle alone (Figure 1d), confirming that SGL-S23–mediated suppression of K/BxN serum transfer arthritis requires iNKT cells.

In addition to visual scoring, we analyzed the histologic features in the joints of all 4 paws in vehicle-treated or SGL-S23–treated mice, on day 10 after disease induction. Quantification of the histologic severity of arthritis is shown in Figure 2a, and typical histologic features are demonstrated in Figures 2b and c. Arthritis was not apparent in the joints of mice treated with SGL-S23 (Figure 2b), in contrast to the severe arthritis with massive cell infiltration, cartilage erosion, and bone destruction seen in the joints of animals treated with vehicle (Figure 2c).

Necessity of IFNγ for SGL-S23–mediated suppression of arthritis. To investigate the mechanism of SGL-S23–mediated suppression of K/BxN serum trans-

Table 1. Clinical arthritis scores in mice with K/BxN serum transfer arthritis*

Treatment	Maximum score	Day of onset
Control rat IgG/vehicle	12.6 ± 1.78	2.6 ± 0.24
Control rat IgG/SGL-S23	5.2 ± 1.24†	4.0 ± 0.55
Anti-IFNγ mAb/vehicle	12.4 ± 1.21	2.4 ± 0.24
Anti-IFNγ mAb/SGL-S23	11.6 ± 1.69	2.2 ± 0.2
Anti-IL-4 mAb/vehicle	12.4 ± 1.67	2.8 ± 0.2
Anti-IL-4 mAb/SGL-S23	6.4 ± 1.12‡	3.0 ± 0.32
Anti-IL-10 mAb/vehicle	14.8 ± 1.15	2.8 ± 0.25
Anti-IL-10 mAb/SGL-S23	6.0 ± 1.38§	3.2 ± 0.66
Control mouse IgG/vehicle	12.0 ± 1.78	1.6 ± 0.25
Control mouse IgG/SGL-S23	6.8 ± 0.97¶	3.6 ± 0.51
Anti-TGFβ mAb/vehicle	13.4 ± 1.17	1.8 ± 0.2
Anti-TGFβ mAb/SGL-S23	6.2 ± 0.92#	2.8 ± 0.73

* C57BL/6 mice were treated with 100 μg/kg of SGL-S23 or vehicle, together with neutralizing monoclonal antibodies (mAb) 3 times, starting on day 0. Values are the mean ± SEM of 5 mice per group, from a single experiment representative of 2 similar experiments. Anti-IFNγ = anti-interferon-γ.
† $P = 0.028$ versus control rat IgG plus vehicle.
‡ $P = 0.027$ versus anti-interleukin-4 (anti-IL-4) mAb plus vehicle.
§ $P = 0.0013$ versus anti-IL-10 mAb plus vehicle.
¶ $P = 0.022$ versus control mouse IgG plus vehicle.
# $P = 0.009$ versus anti-transforming growth factor β (anti-TGFβ) mAb plus vehicle.

fer arthritis, we examined the effect of neutralization of cytokines that have been reported to be implicated in iNKT cell–mediated suppression of experimental autoimmune disease. Previous studies showed that Th2 cytokines such as IL-4 and IL-10 were involved in the suppression of Th1-mediated autoimmune disease in models such as collagen-induced arthritis (CIA), type 1 diabetes in NOD mice, and experimental autoimmune encephalomyelitis (13–17). However, in mice with K/BxN serum transfer arthritis, neutralization of IL-4 or IL-10 did not reverse the protective effect of SGL-S23 against arthritis (Table 1). TGFβ has been reported to be involved in the regulation of K/BxN serum transfer arthritis by iNKT cells (27). However, as was found with IL-4 and IL-10, neutralization of TGFβ did not alter the disease course or the inhibitory effect of SGL-S23 on arthritis (Table 1). In contrast, neutralization of IFNγ unexpectedly, almost completely abolished the inhibitory effect of SGL-S23 (Figure 3a and Table 1).

Inhibition of K/BxN serum transfer arthritis by systemic administration of IFNγ. Since it had not previously been reported that IFNγ suppresses autoantibody-mediated inflammation, we next examined whether administration of IFNγ would ameliorate K/BxN serum transfer arthritis. As shown in Figure 3b, injection of IFNγ reduced the clinical severity of arthritis. Interestingly, there was a tendency for IFNγ administered at a relatively low dose (1 ng) to inhibit arthritis

more effectively compared with higher-dose IFNγ (5 ng or 25 ng).

Biologic function of SGL-S23 in vitro and in vivo. We next compared the ability of SGL-S23 and α-GalCer to stimulate NKT cells isolated from liver mononuclear cells. As observed previously (21), α-GalCer at the lowest dose induced a maximum proliferative response (Figure 4a). In contrast, SGL-S23 was able to induce proliferation only when used at higher doses, and its efficacy was lower than that of α-GalCer (Figure 4a). In addition, SGL-S23 at a dose of 90 ng/ml was able to induce IFNγ production (mean ± SEM 21.3 ± 1.40 ng/ml), even though its efficacy was much lower compared with α-GalCer stimulation (830 ± 72.7 pg/ml). The response of liver-derived mononuclear cells to SGL-S23 or to α-GalCer was completely abolished in iNKT cell–deficient TCR $J_\alpha18$–knockout mice (data not shown), indicating that the response to SGL-S23 is mediated by iNKT cells. S25 or S27 did not induce IFNγ production (data not shown).

Next we examined the response of iNKT cells to SGL-S23 in vivo. We injected SGL-S23, S25, S27, or α-GalCer into B6 mice and measured serum levels of IFNγ by ELISA. Consistent with data obtained in vitro, SGL-S23 induced IFNγ to a lesser extent compared with induction by α-GalCer (Figure 4b). IFNγ was not induced in vivo by either S25 or S27.
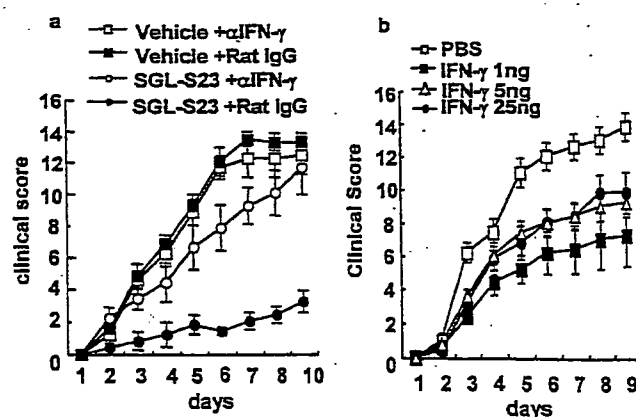

Figure 3. Role of interferon-γ (IFNγ) in SGL-S23–mediated suppression of arthritis. a, Clinical score of K/BxN serum transfer arthritis in C57BL/6 (B6) mice treated with 100 μg/kg of SGL-S23 or vehicle together with anti-IFNγ neutralizing monoclonal antibody (αIFNγ) or control rat IgG 3 times, starting on the day of K/BxN serum transfer (day 0). b, Clinical score of K/BxN serum transfer arthritis in B6 mice treated with phosphate buffered saline (PBS) or with IFNγ administered subcutaneously every day starting on day 0. Values are the mean ± SEM of 5 mice per group, from a single experiment representative of 2 similar experiments.
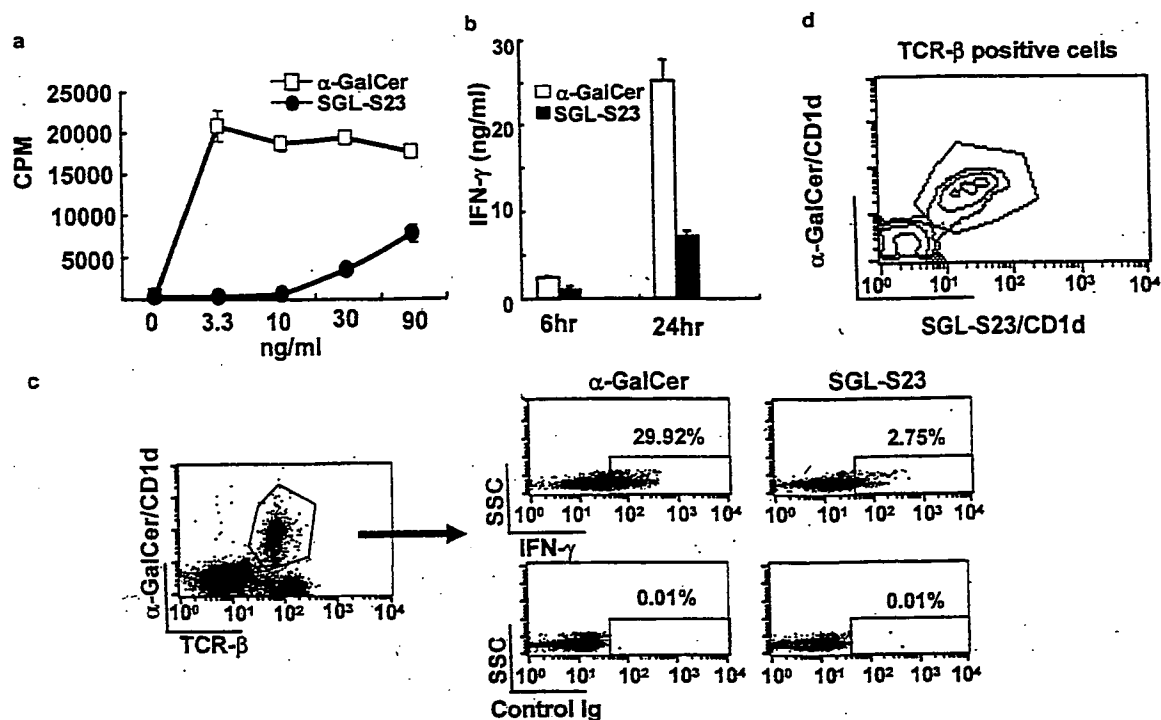
Figure 4. Interferon-γ (IFNγ) production by invariant natural killer T (iNKT) cells stimulated with SGL-S23 in vitro and in vivo. a, Effect of glycolipids on liver-derived NKT cells. NK1.1+,CD3+ cells were sorted from liver mononuclear cells and were cultured with various concentrations of α-galactosylceramide (α-GalCer) or SGL-S23 in the presence of irradiated dendritic cells. Proliferative responses were assessed based on ^{3}H-thymidine incorporation. b, Change in serum IFNγ levels in C57BL/6 mice after injection of glycolipids. Serum levels of IFNγ 6 hours and 24 hours after intravenous injection of glycolipids were measured by enzyme-linked immunosorbent assay. Values in a and b are the mean ± SEM of 3 mice per group, from a single experiment representative of 3 similar experiments. c, IFNγ production by iNKT cells 2 hours after intraperitoneal injection of α-GalCer or SGL-S23. Intracellular IFNγ-containing cells among CD1d–Dimer X–positive, T cell receptor β (TCRβ)–positive iNKT cells were quantified by flow cytometry. d, Results from double staining of TCRβ-positive cells with α-GalCer–loaded CD1d and SGL-S23–loaded CD1d. Data in c and d are from a single experiment representative of 3 similar experiments. SSC = side scatter.

Production of IFNγ by SGL-S23–activated iNKT cells was further confirmed by intracellular staining of IFNγ in iNKT cells derived from liver mononuclear cells after SGL-S23 injection. It has been shown that iNKT cells produce IFNγ mainly at an early time point, such as ~1–2 hours after injection of glycolipid ligands, and lower induction of IFNγ by iNKT cells results in lower levels of IFNγ in serum, mainly mediated by other cells such as NK cells, at later time points, such as ~6–24 hours after ligand injection (23). Therefore, it seemed reasonable that lower initial IFNγ production by iNKT cells would result in lower induction of IFNγ at later time points. We confirmed that SGL-S23–reactive iNKT cells could recognize α-GalCer as well as α-GalCer-reactive iNKT cells, as shown in Figure 4d. This was consistent with the finding that SGL-S23, a weak inducer of IFNγ, was most effective in suppressing arthritis.

Inhibition of mast cell activation by administration of SGL-S23 or IFNγ. A profound decrease of cellular infiltration into the joints of SGL-S23–treated-mice suggested that the mechanisms of SGL-S23–mediated suppression of arthritis involve inhibition of inflammation at an early phase. We examined the expression of C5a receptor, lymphocyte function–associated antigen 1 (LFA-1), and FcγRIII, which have been previously reported to be necessary for the development of K/BxN serum transfer arthritis, on granulocytes and macrophages, critical components of this model of arthritis (6,9,10,31). The expression of C5a receptor, LFA-1, and FcγRIII on these cells was not reduced during the course of arthritis in SGL-S23-treated mice compared with vehicle-treated mice (data not shown).

Mast cells have been shown to be essential for the
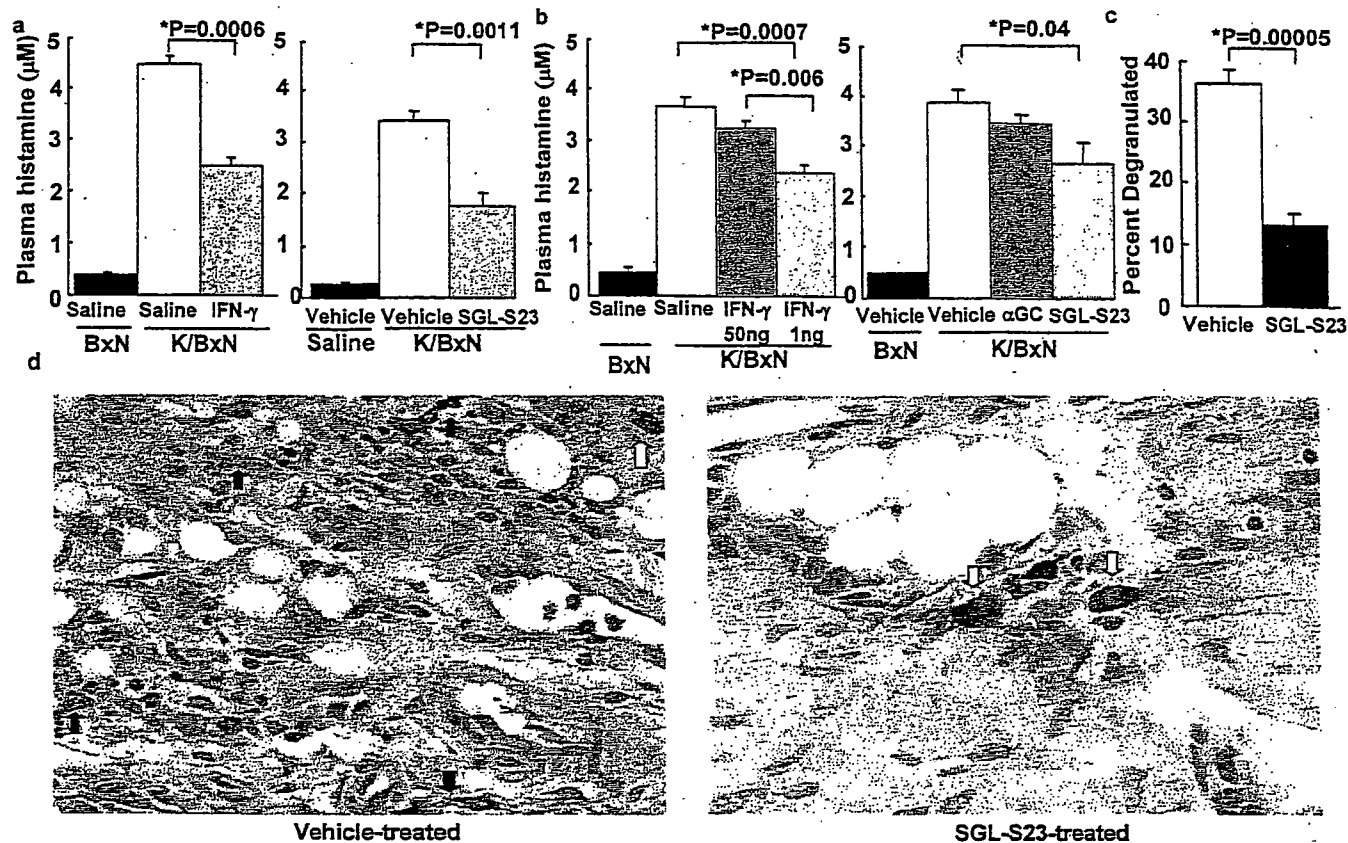
Figure 5. Effect of administration of SGL-S23 on mast cell activation induced by K/BxN serum injection. a (left panel), Plasma histamine concentrations 5 minutes after injection of K/BxN serum in C57BL/6 (B6) mice pretreated for 3 days by subcutaneous injection of phosphate buffered saline (PBS) or interferon-γ (IFNγ). BxN serum was injected as a control. a (right panel), Plasma histamine concentrations 5 minutes after injection of K/BxN serum in B6 mice treated with SGL-S23 or vehicle. PBS was injected as a control. b (left panel), Plasma histamine concentrations 5 minutes after injection of K/BxN serum in B6 mice pretreated for 3 days by subcutaneous injection of IFNγ at the indicated concentrations. b (right panel), Plasma histamine concentrations 5 minutes after injection of K/BxN serum in B6 mice pretreated with SGL-S23 or α-galactosylceramide (αGC). c, Quantification of histopathologic assessment of mast cell activation 10 days after K/BxN serum transfer in SGL-S23–treated or vehicle-treated mice. Consecutive tissue sections (shown in Figure 2) were stained with toluidine blue. Values in a–c are the mean and SEM of 5 mice per group (a and b) or 3 mice per group (c), from a single experiment representative of 2 similar experiments. d, Histopathologic features of degranulated or intact mast cells in the joints of representative vehicle-treated and SGL-S23–treated mice. Solid arrows indicate degranulated mast cells; open arrows indicate intact mast cells (original magnification × 600).

development of arthritis in the K/BxN serum transfer model (8). More recently, vascular leak following mast cell activation induced by K/BxN serum transfer has been shown to be critical for the initiation of arthritis (32). To assess the effect of IFNγ on mast cell activation by serum transfer, we first examined serum level of histamines. B6 mice were treated with 1 ng of IFNγ subcutaneously for 3 consecutive days, and then injected with K/BxN serum intravenously. Five minutes after serum injection, blood was collected and assayed for histamine concentration. As shown in Figure 5a, the plasma histamine concentration increased after treatment with K/BxN serum compared with treatment with

control serum. The elevation of the plasma histamine level was inhibited by administration of IFNγ but not by vehicle administration.

We next examined the effect of SGL-S23 on the increase in plasma histamine levels induced by K/BxN serum injection. B6 mice were pretreated with 100 μg/kg of SGL-S23, and K/BxN serum was injected 24 hours later. Consistent with the result obtained with IFNγ treatment, administration of SGL-S23 also suppressed the plasma level of histamine after transfer of K/BxN serum (Figure 5a). To further investigate the hypothesis that treatment with low-dose IFNγ contributes to the suppression of arthritis, we next determined the differ-

ence in histamine levels after administration of low-dose versus high-dose IFNγ. As shown in Figure 5b, lower-dose IFNγ was more effective in suppressing histamine release. Furthermore, we examined whether SGL-S23 is more effective in suppressing histamine release compared with α-GalCer. As shown in Figure 5b, SGL-S23 suppressed histamine levels more effectively than did α-GalCer after K/BxN serum injection. These results indicate that low-dose IFNγ or SGL-S23 inhibits the release of histamine after K/BxN serum injection, suggesting that suppression of mast cell activation contributes to the inhibition of arthritis development.

To further examine whether mast cells were suppressed in SGL-S23–treated arthritic mice, we performed histologic analysis to evaluate mast cell activation. Because degranulation is the clearest histologic hallmark of mast cell activation, mast cells in the joint sections were visually assessed for intact versus degranulating phenotype in tissues stained with toluidine blue. The proportion of degranulated mast cells was significantly lower in SGL-S23–treated mice compared with vehicle-treated control mice. Taken together, these results indicate that mast cell activation is suppressed in mice treated with SGL-S23.

DISCUSSION

We demonstrated in the present study that a newly synthesized glycolipid ligand for iNKT cells, SGL-S23 (a sphingosine chain elongated analog of α-GalCer), strongly suppressed K/BxN serum transfer arthritis by inhibiting inflammatory cell infiltration and the resultant destruction of cartilage and bone. SGL-S23–mediated suppression of arthritis was dependent on IFNγ. Consistent with this, administration of IFNγ inhibited the development of arthritis. Administration of either SGL-S23 or IFNγ suppressed the K/BxN serum transfer–induced histamine release from mast cells that is critical for the initiation of arthritis.

It has been reported that iNKT cells are involved in the pathogenesis of K/BxN serum transfer arthritis (26,27). Activation of iNKT cells by α-GalCer has been previously shown to exacerbate K/BxN serum transfer arthritis (27), which is inconsistent with our finding in the present study that α-GalCer inhibited arthritis to some extent. It is clear that newly synthesized SGL-S23 inhibited arthritis to a greater extent than did α-GalCer, however, and the reason for the discrepancy between the previous result and ours is not known.

IFNγ has been shown to have biphasic functions in several murine arthritis models, such as CIA,

adjuvant-induced arthritis, and group B streptococcal arthritis (33–36). Administration of IFNγ exacerbated arthritis and blocking of IFNγ inhibited arthritis at an early stage in these models; however, when IFNγ was administered at a later time point, arthritis was not exacerbated, and was in fact suppressed. IFNγ appears to enhance the immune response in the early phase, and to down-regulate arthritis in the later phase in these models. Moreover, acceleration of CIA has been reported in both IFNγ-knockout and IFNγ receptor-knockout mice (37,38). K/BxN serum transfer arthritis is considered to represent the inflammatory process of arthritis; therefore, the suppression of disease by IFNγ observed in the present study is not inconsistent with these previous findings.

Although IFNγ has been shown to have both an enhancing and a suppressive effect on autoimmune inflammation, the mechanisms that underlie the inhibition of inflammation are not clearly understood (39,40). The suppressive effect of IFNγ on osteoclastogenesis has been implicated as one of the mechanisms of inhibition of arthritis (41). Activation-induced cell death of T cells has also been suggested to be involved in IFNγ-mediated suppression of inflammation (42,43). More recently, IFNγ has been shown to suppress the development of IL-17–producing T cells, which are critical for autoimmune inflammation (44–47).

However, it is unlikely that SGL-S23–mediated suppression of K/BxN serum transfer arthritis involves these mechanisms, because lymphocytes are not required for the development of arthritis in this model. Furthermore, the inhibition of arthritis by SGL-S23 is accompanied by suppression of inflammatory cell infiltration into the joints prior to bone destruction by osteoclasts. Therefore, our results suggest that IFNγ-regulated inflammatory cells are involved in innate immune responses. IFNγ is well known as a stimulator of monocyte/macrophages and granulocytes, which are important for the development of K/BxN serum transfer arthritis. In support of this, administration of SGL-S23 did not induce any suppressive effect on these cells. SGL-S23 did, however, reduce the release of histamine induced by K/BxN serum transfer, suggesting suppression of the mast cell activation that is crucial for the development of arthritis.

Interestingly, SGL-S23 is less potent than α-GalCer in stimulating iNKT cells and inducing IFNγ production, which is consistent with the finding that IFNγ suppressed arthritis more effectively at a lower dose than at a higher dose. Similarly, low-dose IFNγ has been demonstrated to prevent migration of T cells and B

cells (48–50). IFNγ might suppress inflammation only if administered at a very precise dosage level, and SGL-S23 may thus have greater utility as an inhibitor of inflammatory arthritis. High, nonphysiologic doses of IFNγ may induce negative feedback loops, thereby limiting any potential protective effects.

We have previously shown that OCH, another analog of α-GalCer with a truncated sphingosine chain, preferentially induces Th2 cytokines (21–23). SGL-S23 administered in vivo induces more IFNγ and less IL-4 compared with OCH and possesses a stronger ability to suppress inflammatory arthritis compared with α-GalCer or OCH (Kaieda S, et al: unpublished observations), indicating a unique property of this ligand. SGL-S23 may have clinical benefit over α-GalCer since it induces a weaker cytokine response in iNKT cells, thereby reducing potential side effects caused by excessive cytokine release. In addition, because repeated administration of SGL-S23 stimulates iNKT cells to a lesser extent than does α-GalCer administration, recovery from nonresponsiveness may be more rapid with SGL-S23 than with α-GalCer.

Manipulation of regulatory cells is a new strategy for immunotherapy, and iNKT cells would serve as one of the most suitable cell types for in vivo stimulation, due to the availability of specific ligands. The lack of polymorphism in the antigen-presenting molecule further indicates that the ligand has potential for widespread use among individuals, unlike major histocompatibility complex–restricted peptide antigens.

ACKNOWLEDGMENTS

AUTHOR CONTRIBUTIONS

Dr. Miyake had full access to all of the data in the study and takes responsibility for the integrity of the data and the accuracy of the data analysis.
Study design. Miyake.
Acquisition of data. Kaieda, Tomi.
Analysis and interpretation of data. Kaieda, Oki, Yamamura, Miyake.
Manuscript preparation. Kaieda, Miyake.
Statistical analysis. Kaieda.

REFERENCES

1. Feldmann M, Brennan FM, Maini RN. Role of cytokines in rheumatoid arthritis. Annu Rev Immunol 2002;14:397–440.

2. Feldmann M. Development of anti-TNF therapy for rheumatoid arthritis. Nat Rev Immunol 2002;2:364–71.

3. Kouskoff V, Korganow AS, Duchatelle V, Degott C, Benoist C, Mathis D. Organ-specific disease provoked by systemic autoimmunity. Cell 1996;87:811–26.

4. Korganow AS, Ji H, Mangialaio S, Dchatelle V, Pelanda R, Martin T, et al. From systemic T cell self-reactivity to organ-specific autoimmune disease via immunoglobulins. Immunity 1999;10: 451–61.

5. Matsumoto I, Staub A, Benoist C, Mathis D. Arthritis provoked by linked T and B cell recognition of a glycolytic enzyme. Science 1999;286:1732–5.

6. Ji H, Ohmura K, Mahmood U, Lee DM, Hofhuis FM, Boackle SA, et al. Arthritis critically dependent on innate immune system players. Immunity 2002;16:157–68.

7. Ji H, Pettit A, Ohmura K, Ortiz-Lopez A, Duchatelle V, Degott C, et al. Critical roles for interleukin 1 and tumor necrosis factor α in antibody-induced arthritis. J Exp Med 2002;196:77–85.

8. Lee DM, Friend DS, Gurish MF, Benoist C, Mathis D, Brenner MB. Mast cells: a cellular link between autoantibodies and inflammatory arthritis. Science 2002;297:1689–92.

9. Wipke BT, Allen PM. Essential role of neutrophils in the initiation and progression of a murine model of rheumatoid arthritis. J Immunol 2002;167:1601–8.

10. Solomon S, Rajasekaran N, Jeisy-Walder E, Snapper SB, Illges H. A crucial role for macrophages in the pathology of K/BxN serum-induced arthritis. Eur J Immunol 2005;35:3064–73.

11. Brigl M, Brenner MB. CD1 antigen presentation and T cell function. Annu Rev Immunol 2004;22:817–90.

12. Kronenberg M. Toward an understanding of NKT cell biology: progress and paradoxes. Annu Rev Immunol 2005;23:877–900.

13. Miyake S, Yamamura T. Therapeutic potential of glycolipid ligands for natural killer (NK) T cells in the suppression of autoimmune diseases. Curr Drug Targets Immune Endocr Metabol Disord 2005;5:315–22.

14. Wilson SB, Delovitch L. Janus-like role of regulatory iNKT cells in autoimmune disease and tumour immunity. Nat Rev Immunol 2003;3:211–22.

15. Mars LT, Novak J, Liblau RS, Lehuen A. Therapeutic manipulation of iNKT cells in autoimmunity: modes of action and potential risks. Trends Immunol 2004;25:471–6.

16. Van Kaer L. α-galactosylceramide therapy for autoimmune diseases: prospects and obstacles. Nat Rev Immunol 2005;5:31–42.

17. Yu KOA, Porcelli SA. The diverse functions of CD1d-restricted NKT cells and their potential for immunotherapy. Immmunol Lett 2005;100:42–55.

18. Kawano T, Cui J, Koezuka Y, Toura I, Kaneko Y, Motoki K, et al. CD1d-restricted and TCR-mediated activation of Vα14 NKT cells by glycosylceramides. Science 1997;278:1626–9.

19. Giaccone G, Punt CJ, Ando Y, Ruijter R, Nishi N, Peters M, et al. A phase I study of the natural killer T-cell ligand α-galactosylceramide (KRN7000) in patients with solid tumors. Clin Cancer Res 2002;8:3702–9.

20. Ishikawa A, Motohashi S, Ishikawa E, Fuchida H, Higashino K, Otsuji M, et al. A phase I study of α-galactosylceramide (KRN7000)-pulsed dendritic cells in patients with advanced and recurrent non-small cell lung cancer. Clin Cancer Res 2005;11: 1910–7.

21. Miyamoto K, Miyake S, Yamamura T. A synthetic glycolipid prevents autoimmune encephalomyelitis by inducing Th2 bias of natural killer T cells. Nature 2001;413:531–4.

22. Oki S, Chiba A, Yamamura T, Miyake S. The clinical implication and molecular mechanism of preferential IL-4 production by modified glycolipid-stimulated NKT cells. J Clin Invest 2004;113: 1631–40.

23. Oki S, Tomi C, Yamamura T, Miyake S. Preferential Th2 polarization by OCH is supported by incompetent NKT cell induction

of CD40L and following production of inflammatory cytokines by bystander cells in vivo. Int Immunol 2005;17:1619–29.

24. Mizuno M, Masumura M, Tomi C, Chiba A, Oki S, Yamamura T, et al. Synthetic glycolipid OCH prevents insulitis and diabetes in NOD mice. J Autoimmun 2004;23:293–300.

25. Chiba A, Oki S, Miyamoto K, Hashimoto H, Yamamura T, Miyake S. Suppression of collagen-induced arthritis by natural killer T cell activation with OCH, a sphingosine-truncated analog of α-galactosylceramide. Arthritis Rheum 2004;50:305–13.

26. Chiba A, Kaieda S, Oki S, Yamamura T, Miyake S. The involvement of V_a14 natural killer T cells in the pathogenesis of arthritis in murine models. Arthritis Rheum 2005;52:1941–8.

27. Kim HY, Kim HJ, Min HS, Park ES, Park SH, Chung DH. NKT cells promote antibody-induced arthritis by suppressing transforming growth factor β1 production. J Exp Med 2005;201:41–7.

28. Cui J, Shin T, Kawano T, Sato H, Kondo E, Toura I, et al. Requirement for Vα14 NKT cells in IL-12-mediated rejection of tumors. Science 1997;278:1623–6.

29. Murata K, Toba T, Nakanishi K, Takahashi B, Yamamura T, Miyake S, et al. Total synthesis of an immunosuppressive glycolipid, (2S,3S,4R)-1-O-(α-d-galactosyl)-2-tetracosanoylamino-1,3,4-nonanetriol. J Org Chem 2005;70:2398–401.

30. Williams RO, Feldmann M, Maini RN. Anti-tumor necrosis factor ameliorates joint disease in murine collagen-induced arthritis. Proc Natl Acad Sci U S A 1992;89:9784–8.

31. Watts GM, Beurskens FJ, Martin-Padura I, Ballantyne CM, Klickstein LB, Brenner MB, et al. Manifestations of inflammatory arthritis are critically dependent on LFA-1. J Immunol 2005;174:3668–75.

32. Binstadt BA, Patel PR, Alencar H, Nigrovic PA, Lee DM, Mahmood U, et al. Particularities of the vasculature can promote the organ specificity of autoimmune attack. Nat Immunol 2006;7:284–92.

33. Boissier MC, Chiocchia G, Bessis N, Hajnal J, Gianni G, Nicolett F, et al. Biphasic effect of interferon-γ in murine collagen-induced arthritis. Eur J Immunol 2006;25:1184–90.

34. Jacob CO, Holoshitz J, van der Meide PH, Strober S, McDevitt HO. Heterogeneous effects of IFN-γ in adjuvant arthritis. J Immunol 1989;142:1500–5.

35. Wiesenberg I, van der Meide PH, Schellekens H, Alkan SS. Suppression and augmentation of rat adjuvant arthritis with monoclonal anti-interferon-γ antibody. Clin Exp Immunol 1989;78:245–9.

36. Puliti M, von Humolstein C, Bistoni F, Mosci P, Orefici G, Tissi L. Influence of interferon-γ administration on the severity of experimental group B streptococcal arthritis. Arthritis Rheum 2000;43:2678–86.

37. Manoury-Schwartz B, Chiocchia G, Bessis N, Abehsira-Amar O,

38. Batteux F, Muller S, et al. High susceptibility to collagen-induced arthritis in mice lacking IFN-γ receptors. J Immunol 1997;158:5501–6.

38. Vermeire K, Heremans H, Vandeputte M, Huang S, Billiau A, Matthys P. Accelerated collagen-induced arthritis in IFN-γ receptor-deficient mice. J Immunol 1997;158:5507–13.

39. Boehm U, Klamp T, Groot M, Howard JC. Cellular responses to interferon-γ. Annu Rev Immunol 1997;15:749–95.

40. Schroder K, Hertzog PJ, Ravasi T, Hume DA. Interferon-γ: an overview of signals, mechanisms and functions. J Leukoc Biol 2004;75:163–89.

41. Takayanagi H, Ogasawara K, Hida S, Chiba T, Murata S, Sato K, et al. T-cell-mediated regulation of osteoclastogenesis by signaling cross-talk between RANKL and IFN-γ. Nature 2000;408:600–5.

42. Cuo CO, Wittmer S, Dalton DK. Failure to suppress the expansion of the activated CD4 T cell population in interferon γ-deficient mice leads to exacerbation of experimental autoimmune encephalomyelitis. J Exp Med 2000;192:123–8.

43. Furlan R, Brambilla E, Ruffini F, Poliani PL, Bergamik A, Marconi PC, et al. Intrathecal delivery of IFN-γ protects C57BL/6 mice from chronic-progressive experimental autoimmune encephalomyelitis by increasing apoptosis of central nervous system-infiltrating lymphocytes. J Immunol 2001;167:1821–9.

44. Veldhoen M, Hocking RJ, Atkins CJ, Locksley RM, Sockinger B. TGFβ in the context of an inflammatory cytokine milieu supports de novo differentiation of IL-17-producing T cells. Immunity 2006;24:179–89.

45. Chen Y, Langrish CL, McKenzie B, Joyce-Shaikh B, Stumhofer JS, McClanahan T, et al. Anti-IL-23 therapy inhibits multiple inflammatory pathways and ameliorates autoimmune encephalomyelitis. J Clin Invest 2006;116:1317–26.

46. Mangan PR, Harrington LE, O'Quinn DB, Helms WS, Bullard DC, Elson CO, et al. Transforming growth factor-β induces development of the Th17 lineage. Nature 2006;441:231–4.

47. Bettelli E, Carrier Y, Gao W, Korn T, Strom TB, Oukka M, et al. Reciprocal developmental pathways for the generation of pathogenic effector Th17 and regulatory T cells. Nature 2006;441:235–8.

48. Flaishon L, Topilski I, Shoseyov D, Hershkoviz R, Fireman E, Levo Y, et al. Anti-inflammatory properties of low levels of IFN-γ. J Immunol 2002;168:3707–11.

49. Flaishon L, Hershkoviz R, Lantner F, Lider O, Alon R, Levo Y, et al. Autocrine secretion of interferon γ negatively regulates homing of immature B cells. J Exp Med 2000;192:1381–8.

50. Flaishon L, Lantner F, Hershkovi R, Levo Y, Shachar I. Low levels of IFN-γ down-regulate the integrin-dependent adhesion of B cells by activating a pathway that interferes with cytoskeleton rearrangement. J Biol Chem 2001;276:46701–6.

CUTTING EDGE

Cutting Edge: Human Th17 Cells Are Identified as Bearing CCR2$^+$CCR5$^-$ Phenotype[1]

Wakiro Sato, Toshimasa Aranami, and Takashi Yamamura[2]

Recent reports have shown that IL-17-producing CD4$^+$ T cells (Th17 cells) belong to a distinct helper T cell lineage and are critically involved in the pathogenesis of autoimmune diseases and allergies. However, the chemokine receptor profile of Th17 cells remains to be clarified. In this study, we report that human Th17 cells are identified as CCR2$^+$CCR5$^-$ memory CD4$^+$ T cells. Analysis of PBMC from healthy donors showed that CCR2$^+$ cells produce much larger amounts of IL-17 than CCR2$^-$ cells, indicating the preferential expression of CCR2 on Th17 cells. Notably, CCR2$^+$CCR5$^-$ memory CD4$^+$ T cells produced a large amount of IL-17 and little IFN-γ, whereas CCR2$^+$CCR5$^+$ cells reciprocally produced an enormous amount of IFN-γ but little IL-17. Moreover, a higher expression of T-bet was seen in the CCR5$^+$ memory T cells. These results indicate that absence of CCR5 distinguishes human Th17 cells from Th1 cells. The Journal of Immunology, 2007, 178: 7525–7529.

CD4$^+$ Th cells are essential regulators of adaptive immune responses. Th cells have been classified as either Th1 or Th2 according to the cytokine production profile and functional properties. However, recent studies have demonstrated that IL-17-producing T cells, rather than Th1 cells, play a pivotal role in the pathogenesis of autoimmune disease models, including experimental autoimmune encephalomyelitis (EAE)[3] (1–4). IL-17 is a cytokine mainly produced by activated memory T cells and could recruit and expand neutrophils through induction of various chemokines and GM-CSF (5–7).

Numerous studies have provided evidence that IL-17-producing T cells belong to a distinct lineage of Th cells whose development is severely hampered in IL-23 knockout but not in IL-12 knockout mice (8, 9). Although IL-23 was initially thought to induce differentiation of the IL-17-producing cells, it now seems that IL-23 is not involved in differentiation but

propagation of Th17 cells (10). In fact, recent studies have shown that a combination of TGF-β1 plus IL-6 promotes the differentiation of Th17 cells in vitro (11–13). Differentiation of Th17 cells is prohibited by IFN-γ or IL-4 (11–13), further supporting the concept that Th17 cells comprise a distinct population cross-regulated by Th1 or Th2 cells. Notably, the independent nature of Th17 cells has been further highlighted by the recent discovery that the transcription factor RORγt is critically involved in the development of Th17 cells (14).

During the critical process whereby naive CD4$^+$ T cells differentiate, they acquire reciprocal sets of chemokine receptors (15), which would endow them a unique character of homing or migration to corresponding ligand chemokines. Namely, Th1 cells preferentially express CCR5 and CXCR3 and migrate to inflammatory milieu expressing the corresponding ligand chemokines, whereas Th2 cells express CCR4, CCR8, and CRTh2 indicative of a distinctive homing property (16–19). It is conceivable that Th17 cells may also possess unique chemotactic and migratory property. However, chemokine receptor expression by Th17 cells has not been characterized yet, at least to our knowledge.

In this study, we attempted to identify chemokine receptor expression by human Th17 cells by examining cytokine production profiles of T cell subpopulation-bearing chemokine receptor(s) of interest (16, 20). We started by comparing CCR2$^+$ and CCR2$^-$ memory CD4$^+$ T cells, because CCR2 and its ligand CCL2 were shown to be essential for development of EAE (21, 22). We found that only the CCR2$^+$ subpopulation would produce IL-17. Further analysis has demonstrated that CCR5$^-$ cells among the CCR2$^+$CD4$^+$ memory T cells produce IL-17, whereas a CCR5$^+$ subpopulation produces IFN-γ. Thus, human Th17 cells are identified as uniquely bearing the CCR2$^+$CCR5$^-$ phenotype.

Materials and Methods

Reagents

Anti-CCR2-biotin mAb, anti-CCR5-FITC mAb, and goat anti-IL-23R polyclonal Abs were purchased from R&D Systems. Streptavidin-PE, anti-CD4-PC5 mAb, and anti-CD45RA-energy-coupled dye (ECD) mAb were obtained from Beckman Coulter, anti-CCR5-allophycocyanin mAb from BD Pharmingen, and donkey anti-goat IgG-FITC from Jackson ImmunoResearch Laboratories. Anti-T-bet mAb and isotype control Ab (mouse IgG1a) purchased from Santa Cruz Biotechnology were used for intracellular staining. RPMI 1640 medium (Invitrogen Life Technologies) was supplemented with 0.05 mM 2-ME, 2 mM L-glutamine, 100 U/ml penicillin/streptomycin, and 10% FBS.

Cell preparation

Peripheral blood was obtained from healthy human volunteers (24–42 years of age) from whom informed consent was obtained. The Ethics Committee of the National Center of Neurology and Psychiatry approved the study. PBMC were freshly isolated by density gradient centrifugation using Ficoll-Paque Plus (Amersham Biosciences). To purify whole T cells or memory CD4$^-$ T cells from PBMC, we used a Pan T cell isolation kit II or Memory CD4$^-$ T cell isolation kit (Miltenyi Biotec), respectively. Briefly, PBMC were labeled with a mixture of biotin-conjugated mAbs directed against either non-T or non-memory CD4$^+$ T cells and then reacted with magnetic microbead-conjugated anti-biotin mAbs. The magnetically labeled non-T or non-memory CD4$^-$ T cells were depleted with autoMACS (Miltenyi Biotec), which yielded >95% purity of whole T cells or memory CD4$^+$ T cells as assessed by flow cytometry for the proportion of CD3$^-$ cells or CD4$^-$CD45RA$^-$ cells.

To further separate the purified cells according to CCR2 or CCR5 expression, they were labeled with anti-CCR2-biotin, streptavidin-PE, and anti-PE microbeads (Miltenyi Biotec) or anti-CCR5-FITC and anti-FITC microbeads (Miltenyi Biotec). The magnetically labeled cells were separated into positive (CCR2$^+$ and CCR5$^+$) and negative (CCR2$^-$ and CCR5$^-$) fractions with autoMACS (>99% purity of CCR2 $^-$or CCR5$^-$ cells and >90% purity of CCR2$^+$ or CCR5$^+$ cells). To obtain CCR2$^+$CCR5$^-$ and CCR2$^-$CCR5$^-$ memory CD4$^-$ T cells, CCR2$^+$ memory CD4$^-$ T cells were labeled with anti-CCR5-allophycocyanin and separated into CCR2$^+$CCR5$^-$ (>80% purity) and CCR2$^-$CCR5$^+$ cells (>95% purity) by flow cytometric cell sorter Epics Altra (Beckman Coulter).

Cell culture and cytokine measurement by ELISA

Purified T cell populations were resuspended at 5 × 10^5/ml and stimulated with PMA (50 ng/ml) and ionomycin (1 µg/ml) in 96-well U-bottom plates for 24 h. The concentrations of IFN-γ and IL-17 in the supernatants were measured by using a Human IFN-γ ELISA Set (BD Pharmingen) and a Human IL-17 DuoSet (R&D Systems).

Flow cytometric analysis of chemokine receptors

To evaluate the expression of chemokine receptors, purified memory CD4$^+$ T cells were stained with anti-CD4-PC5, anti-CD45RA-ECD, anti-CCR5-FITC and PE-conjugated mAbs against anti-CCR2-biotin were analyzed with Epics flow cytometry (Beckman Coulter). To examine the expression of IL-23R, memory CD4$^-$ T cells were stained with goat anti-IL-23R and anti-goat-IgG-FITC and were analyzed with a FACSCalibur (BD Pharmingen).

Intracellular staining of T-bet

Purified memory CD4$^+$ T cells were first stained with biotin-conjugated anti-CCR2, streptavidin-PE, and allophycocyanin-CCR5, then fixed in PBS containing 2% paraformaldehyde and permeabilized with 0.1% saponin solution. Subsequently, the cells were stained with FITC-anti-T-bet. Mouse IgG1a was used as an isotype control.

Statistics

An unpaired Student's t test or one-way ANOVA was used for statistical analysis. We considered $p < 0.01$ as significant.

Results and Discussion

Both Th17 cells and Th1 cells are enriched in CCR2$^+$ CD4$^-$ memory T cells

Previous reports on the CCR2 requirement for development of EAE (21, 22) prompted us to compare the cytokine-producing ability of CCR2$^+$ and CCR2$^-$ cells isolated from whole T cells. The results showed that CCR2$^+$ cells produced a larger amount of IFN-γ and IL-17 as compared with CCR2$^-$ cells, whereas

unseparated whole T cells showed intermediate values (Fig. 1*A*, *upper panels*). This indicates that CCR2$^-$ cells contain the vast majority of Th1 and Th17 cells. We next separated the whole T cells into CCR5$^+$ and CCR5$^-$ populations to compare the cytokine profile. Although CCR5$^+$ cells produced a larger amount of IFN-γ as compared with CCR5$^-$ or the whole T
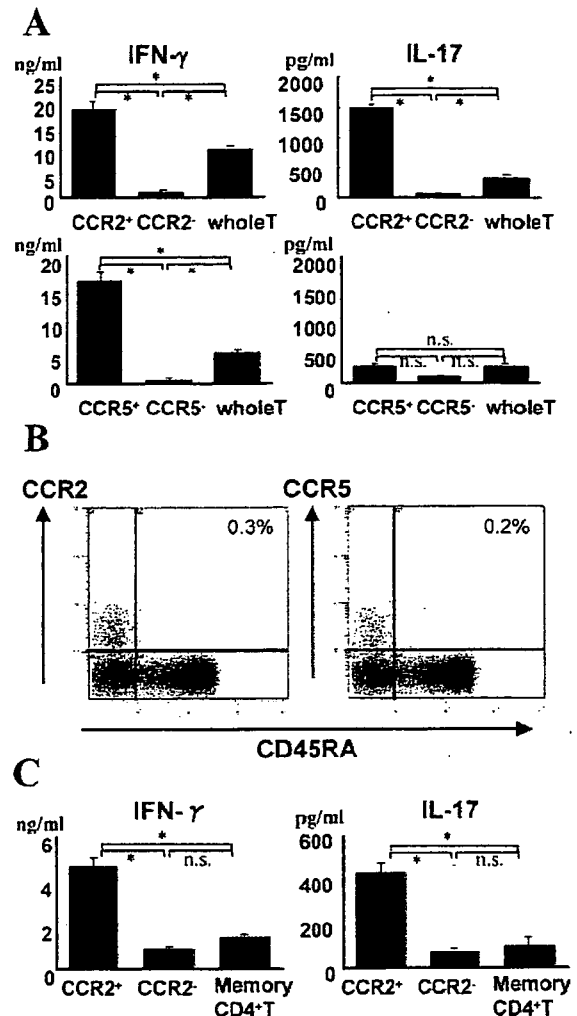

FIGURE 1. Th17 cells are enriched in CCR2$^+$CD4$^-$CD45RA$^-$ cells. *A*, IL-17-producing cells are selectively enriched in the CCR2$^-$, but not in a CCR5$^+$ population. From PBMC of healthy donors, whole T cells were purified magnetically by negative selection using a Pan T cell isolation kit II with autoMACS. The purity of the cells was generally >98%, as determined by FACS analysis. Purified CCR2$^+$ and CCR2$^-$ T cells (or CCR5$^+$ and CCR5$^-$ T cells) were stimulated with PMA and ionomycin for 24 h before the supernatants were collected. The IFN-γ and IL-17 protein in each supernatant was measured using ELISA. Results are expressed as mean ± SD of a representative of five independent experiments. *B*, Chemokine receptor (CCR2 or CCR5) expressing T cells are largely confined to CD45RA$^-$ memory T cells. PBMC from healthy subjects were stained with anti-CCR2 (PE), anti-CCR5 (FITC), anti-CD4 (PC5), and anti-CD45RA (ECD) and analyzed after being gated for CD4. Shown is a representative of five individual data sets. *C*, Th17 cells are enriched in CCR2$^+$CD4$^-$CD45RA$^-$ cells. Memory CD4$^+$ T cells were purified by a memory CD4$^+$ T cell isolation kit with autoMACS. CCR2$^+$ and CCR2$^-$ T cells were further isolated by anti-CCR2-biotin, streptavidin-PE, anti-PE microbeads, and autoMACS. Purified cells were stimulated with PMA and ionomycin for 24 h before collecting supernatants. Results are expressed as mean ± SD of a representative of five independent experiments. *, $p < 0.01$.

cells (Fig. 1A, *lower panels*), production of IL-17 did not increase after enrichment for CCR5$^+$ cells. These results suggest that Th17 cells may be selectively enriched in CCR2$^-$, but not in CCR5$^-$ populations. However, because the CCR2$^+$ T cell preparation also contains CD8$^+$ T cells and γδT cells, capable of producing IL-17 (23–25), it remained possible that the major source of IL-17 could be CD8$^-$ T or γδT cells. Therefore, we next needed to assess the production of IFN-γ and IL-17 from purified CD4$^+$ T cells. Preparatory experiments showed that CCR2$^+$ or CCR5$^+$CD4$^-$ populations are mainly confined to the CD45RA$^-$ memory T cell population (Fig. 1B). Consequently, we decided to use memory CD4$^+$ T cells that could be obtained after deleting CD8$^+$, γδ, and naive CD4$^+$ T cells for further analysis. Analysis of the purified memory CD4$^+$ T cells has also demonstrated that the CCR2$^+$ population produced a significantly larger amount of both IFN-γ and IL-17 compared to the CCR2$^-$ population, with the values of unseparated cells being intermediate (Fig. 1C). These results strongly indicate that Th17 cells as well as Th1 cells are enriched in CCR2$^+$CD4$^+$ memory T cells. However, since Th1 and Th17 cells are thought to belong to distinct T cell lineages, we speculated that they might be further divided into two subpopulations based on expression of chemokine receptors.

CCR2$^+$CCR5$^-$ memory CD4$^+$ T cells predominantly produce IL-17 but not IFN-γ

Simultaneous staining of CCR2 and CCR5 showed that the CCR2$^+$ memory T cell population could be divided into CCR5$^-$ (CCR2 single positive (SP)) and CCR5$^+$ (CCR2 and CCR5 double positive (DP)) subpopulations (Fig. 2). Since CCR5 is reported to be expressed predominantly on Th1 cells (16–18), we hypothesized that SP and DP cells might correspond to Th17 and Th1 cells, respectively. To correlate cytokine production profile and chemokine receptor expression in T cell populations, we first thought of staining total unseparated T cells to detect intracellular cytokines as well as surface CCR; however, the cell activation process required for intracellular cytokine staining was found to down-regulate CCR2 and CCR5 significantly (data not shown), as reported previously (26). To accurately correlate the expression of CCR2 or CCR5
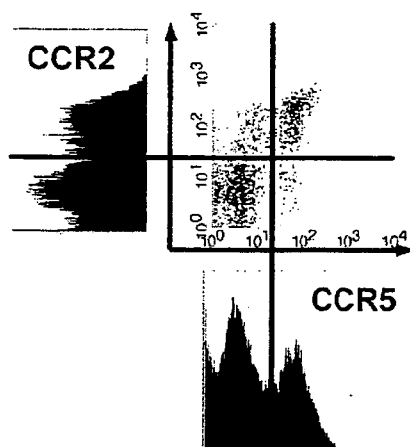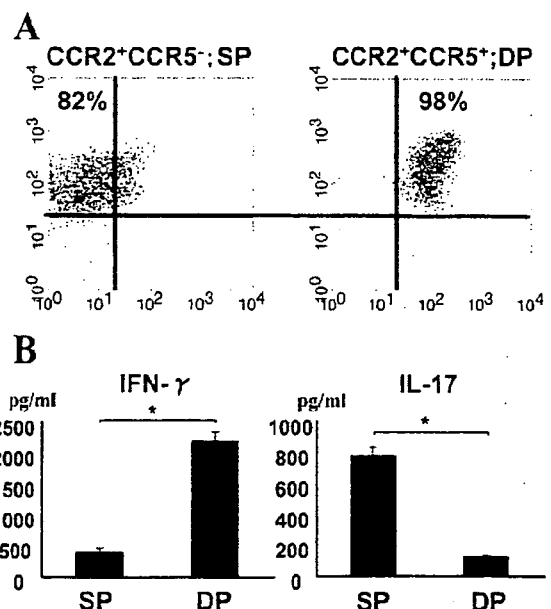
with the cytokine profile ex vivo, we decided to first isolate SP and DP cells from memory CCR2$^+$ T cells by using a flow cytometric cell sorter and stimulate them with PMA and ionomycin. We then measured IFN-γ and IL-17 in the supernatant (Fig. 3A). Remarkably, the sorted T cell subpopulations exhibited different cytokine production patterns: SP cells produced a large amount of IL-17 and a small amount of IFN-γ, whereas DP cells produced a small amount of IL-17 and a large amount of IFN-γ (Fig. 3B). These results suggest that Th17 cells are largely confined to SP cells, whereas DP cells contain a majority of Th1 cells.

T-bet and IL-23R expression in memory CD4$^+$ T cells

Finally, we assessed whether SP and DP cells are distinctive in expression of transcription factor T-bet and IL-23R. T-bet is an essential transcription factor for Th1 differentiation (27), whereas it was reported to be redundant for Th17 cells (3, 8, 9, 11, 14). IL-23 has been shown to play a pivotal role in the survival and expansion of Th17 cells (2, 10). Magnetically purified memory CD4$^+$ T cells were first stained with biotin-conjugated CCR2, streptavidin-PE, and allophycocyanin-CCR5, and then were intracellularly stained with FITC-anti-T-bet or were stained with goat anti-IL-23R Ab and anti-goat IgG-FITC. We compared T-bet expression in SP vs DP cells by evaluating the mean fluorescence intensity (MFI) (Fig. 4, A and B). T-bet was significantly expressed by SP as well as CCR2$^-$CCR5$^-$ double-negative (DN) cells, but its expression was much higher in DP cells and CCR2$^-$CCR5$^+$ cells, suggesting that Th1 cells may be confined to CCR5$^+$ populations. On the other hand, the frequency of IL-23R$^+$ cells was highest in the SP fraction, compared with the others (Fig. 4, C and D).

FIGURE 2. CCR2$^+$ memory CD4$^-$ T cells consist of CCR5$^+$ and CCR5$^-$ subsets. Purified memory CD4$^-$ T cells were stained with anti-CCR2-biotin and streptavidin-PE as well as anti-CCR5-FITC. The separation of positive and negative populations was determined by histogram plots.


FIGURE 3. CCR2$^+$CCR5$^-$ (SP) and CCR2$^+$CCR5$^-$ (DP) cells correspond to Th17 and Th1 cells, respectively. SP and DP subsets were sorted from memory CD4$^+$ T cells by flow cytometry and stimulated with PMA/ionomycin. A, A representative of five individual data sets showing the purity of the sorted cells. B, SP and DP cells were stimulated with PMA/ionomycin for 24 h. Then the amounts of IFN-γ and IL-17 in the supernatant were measured using ELISA. Results are expressed as mean ± SD of a representative of five independent experiments. *, p < 0.01

A

B

C

D
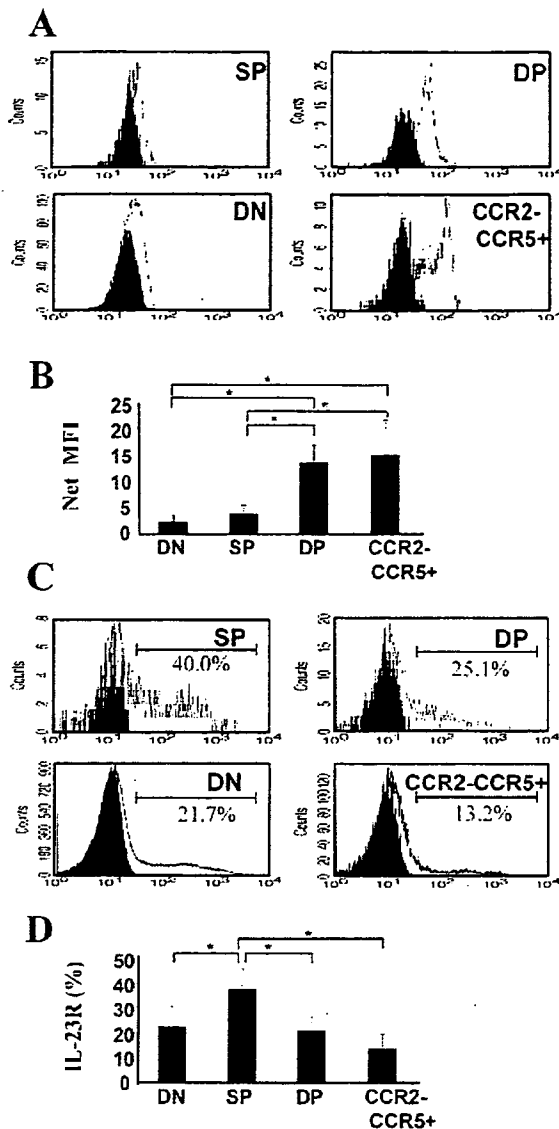
FIGURE 4. T-bet expression of memory CD4⁻ T cells. *A*, Histogram plots of T-bet expression within memory CD4⁺ T cells. SP, DP, DN (CCR2⁻CCR5⁻), and CCR2⁻CCR5⁺ T cells were stained with anti-T-bet or isotype control Ab. Shown is a representative of five individual data sets. *B*, The MFI of each histogram plot. Data for the MFI of T-bet expression subtracted by that of control Ab are calculated and shown as bar graphs with error bars showing the SD of four individual data sets. *C*, Histogram plots of IL-23R expression within memory CD4⁻ T cells. The cells were stained with goat anti-IL-23R polyclonal Ab and anti-goat-FITC Ab. A representative of seven individual data sets is shown. *, p < 0.01. *D*, The frequency of IL-23R-positive cells of each histogram plot. Data are shown as bar graphs with error bars showing the SD of seven individual data sets. *, p < 0.01.

Given the distinguished ability to produce IL-17 as well as higher IL-23R and lower T-bet expression, we propose that Th17 cells are confined to SP cells, whereas Th1 cells are either DP or CCR2⁻CCR5⁺. It has recently been reported that T-bet directly regulates the transcription of IL-23R in mice (28). It is possible that weak expression of IL-23R by non-Th17 cells (DP, DN, and CCR2⁻CCR5⁺) may result from baseline activation of T-bet.

Additional remarks

Using freshly isolated healthy human lymphocytes, we showed here that CCR2⁺CCR5⁻ memory T cells would produce a large amount of IL-17 but not IFN-γ, whereas CCR2⁻ memory T cells produced IFN-γ, but not IL-17. Although we presented the data obtained after stimulation with PMA/ionomycin, polyclonal stimulation by anti-CD3/CD28 also gave similar results (data not shown). Moreover, when we stimulated CCR2⁺CD4⁻ memory T cells by IFN-γ, IL-4, IL-2, or IL-23 in addition to PMA/ionomycin, IL-17 production was not changed (data not shown).

The frequency of Th17 cells among this subset is an important issue to be investigated. By using the ELISPOT assay, we found that ~200 spots of IL-17-producing cells could be detected among 1 × 10⁵ memory CCR2⁻CD4⁺ T cells (~0.2%), whereas the numbers of IFN-γ-producing cells were about 5-fold higher (~1.0%). Although this needs to be systematically verified, the lower frequency of IL-17-producing cells is consistent with the lower value of IL-17 than IFN-γ in supernatants detected by ELISA.

The unique chemokine receptor expression pattern of Th17 cells provides a basis for their recruitment to specialized inflammatory conditions in vivo, which should be relevant for understanding the pathogenesis of autoimmune diseases.

Acknowledgments

Disclosures

The authors have no financial conflict of interest.

References

1. Cua, D. J., J. Sherlock, Y. Chen, C. A. Murphy, B. Joyce, B. Seymour, L. Lucian, W. To, S. Kwan, T. Churakova, et al. 2003. Interleukin-23 rather than interleukin-12 is the critical cytokine for autoimmune inflammation of the brain. *Nature* 421: 744–748.
2. Langrish, C. L., Y. Chen, W. M. Blumenschein, J. Mattson, B. Basham, J. D. Sedgwick, T. McClanahan, R. A. Kastelein, and D. J. Cua. 2005. IL-23 drives a pathogenic T cell population that induces autoimmune inflammation. *J. Exp. Med.* 201: 233–240.
3. Chen. Y., C. L. Langrish, B. McKenzie, B. Joyce Shaikh, J. S. Stumhofer, T. McClanahan, W. Blumenschein, T. Churakovsa, J. Low, L. Presta, et al. 2006. Anti-IL-23 therapy inhibits multiple inflammatory pathways and ameliorates autoimmune encephalomyelitis. *J. Clin. Invest.* 116: 1317–1326.
4. Yen, D., J. Cheung, H. Scheerens, F. Poulet, T. McClanahan, B. McKenzie, M. A. Kleinschek, A. Owyang, J. Mattson, W. Blumenschein, et al. 2006. IL-23 is essential for T cell-mediated colitis and promotes inflammation via IL-17 and IL-6. *J. Clin. Invest.* 116: 1310–1316.
5. Yao. Z., S. L. Painter, W. C. Fanslow, D. Ulrich, B. M. Macduff, M. K. Spriggs, and R. J. Armitage. 1995. Human IL-17: a novel cytokine derived from T cells. *J. Immunol.* 155: 5483–5486.
6. Kolls, J. K., and A. Linden. 2004. Interleukin-17 family members and inflammation. *Immunity* 21: 467–476.
7. Stark, M. A., Y. Huo, T. L. Burcin, M. A. Morris, T. S. Olson, and K. Ley. 2005. Phagocytosis of apoptotic neutrophils regulates granulopoiesis via IL-23 and IL-17. *Immunity* 22: 285–294.
8. Harrington, L. E., R. D. Hatton, P. R. Mangan, H. Turner, T. L. Murphy, K. M. Murphy, and C. T. Weaver. 2005. Interleukin 17-producing CD4⁺ effector T cells develop via a lineage distinct from the T helper type 1 and 2 lineages. *Nat. Immunol.* 6: 1123–1132.
9. Park, H., Z. Li, X. O. Yang, S. H. Chang, R. Nurieva, Y. H. Wang, Y. Wang, L. Hood, Z. Zhu, Q. Tian, and C. Dong. 2005. A distinct lineage of CD4 T cells regulates tissue inflammation by producing interleukin 17. *Nat. Immunol.* 6: 1133–1141.
10. Aggarwal, S., N. Ghilardi, M. H. Xie, F. J. de Sauvage, and A. L. Gurney. 2003. Interleukin-23 promotes a distinct CD4 T cell activation state characterized by the production of interleukin-17. *J. Biol. Chem.* 278: 1910–1914.
11. Veldhoen, M., R. J. Hocking, C. J. Atkins, R. M. Locksley, and B. Stockinger. 2006. TGFβ in the context of an inflammatory cytokine milieu supports de novo differentiation of IL-17-producing T cells. *Immunity* 24: 179–189.
12. Bettelli, E., Y. Carrier, W. Gao, T. Korn, T. B. Strom, M. Oukka, H. L. Weiner, and V. K. Kuchroo. 2006. Reciprocal developmental pathways for the generation of pathogenic effector TH17 and regulatory T cells. *Nature* 441: 235–238.
13. Mangan, P. R., L. E. Harrington, D. B. O'Quinn, W. S. Helms, D. C. Bullard, C. O. Elson, R. D. Hatton, S. M. Wahl, T. R. Schoeb, and C. T. Weaver. 2006.